



SCUOLA INTERNAZIONALE SUPERIORE DI STUDI AVANZATI

SISSA Digital Library

Measuring α in the early universe: Cosmic microwave background polarization, re-ionization and the Fisher matrix analysis

Original

Measuring α in the early universe: Cosmic microwave background polarization, re-ionization and the Fisher matrix analysis / Rocha, G.; Trotta, R.; Martins, C. J. A. P.; Melchiorri, A.; Avelino, P. P.; Bean, R.; Viana, P. T. P.. - In: MONTHLY NOTICES OF THE ROYAL ASTRONOMICAL SOCIETY. - ISSN 0035-8711. - 352:1(2004), pp. 20-38. [10.1111/j.1365-2966.2004.07832.x]

Availability:

This version is available at: 20.500.11767/116859 since: 2020-12-30T22:25:38Z

Publisher:

Published

DOI:10.1111/j.1365-2966.2004.07832.x

Terms of use:

Testo definito dall'ateneo relativo alle clausole di concessione d'uso

Publisher copyright

note finali coverpage

(Article begins on next page)

Measuring α in the Early Universe: CMB Polarization, Reionization and the Fisher Matrix Analysis

G. Rocha,^{1,2,*} R. Trotta,^{3,†} C.J.A.P. Martins,^{2,4,5,‡} A.
Melchiorri,^{6,7,§} P. P. Avelino,^{8,¶} R. Bean,^{9,**} and P.T.P. Viana^{2,10,††}

¹*Astrophysics Group, Cavendish Laboratory, Madingley Road, Cambridge CB3 0HE, United Kingdom*

²*Centro de Astrofísica da Universidade do Porto, R. das Estrelas s/n, 4150-762 Porto, Portugal*

³*Département de Physique Théorique, Université de Genève,
24 quai Ernest Ansermet, CH-1211 Genève 4, Switzerland*

⁴*Department of Applied Mathematics and Theoretical Physics, Centre for Mathematical Sciences,
University of Cambridge, Wilberforce Road, Cambridge CB3 0WA, United Kingdom*

⁵*Institut d'Astrophysique de Paris, 98 bis Boulevard Arago, 75014 Paris, France*

⁶*Department of Physics, Nuclear & Astrophysics Laboratory,
University of Oxford, Keble Road, Oxford OX1 3RH, United Kingdom*

⁷*Universita' di Roma "La Sapienza, Ple Aldo Moro 2, 00185, Rome, Italy*

⁸*Centro de Física do Porto e Departamento de Física da Faculdade de Ciências da Universidade do Porto,
Rua do Campo Alegre 687, 4169-007 Porto, Portugal*

⁹*Department of Astrophysical Sciences, Princeton University,
Peyton Hall - Ivy Lane, Princeton NJ08544-1001, U.S.A.*

¹⁰*Departamento de Matemática Aplicada da Faculdade de Ciências da Universidade do Porto,
Rua do Campo Alegre 687, 4169-007 Porto, Portugal*

We present a detailed analysis of present and future Cosmic Microwave Background constraints of the value of the fine-structure constant, α . We carry out a more detailed analysis of the WMAP first-year data, deriving state-of-the-art constraints on α and discussing various other issues, such as the possible hints for the running of the spectral index. We find, at 95% C.L. that $0.95 < \alpha_{\text{dec}}/\alpha_0 < 1.02$. Setting $dn_S/dlnk = 0$, yields $0.94 < \alpha_{\text{dec}}/\alpha_0 < 1.01$ as previously reported. We find that a lower value of α/α_0 makes a value of $dn_S/dlnk = 0$ more compatible with the data. We also perform a thorough Fisher Matrix Analysis (including both temperature and polarization, as well as α and the optical depth τ), in order to estimate how future CMB experiments will be able to constrain α and other cosmological parameters. We find that Planck data alone can constrain τ with an accuracy of the order 4% and that this constraint can be as small as 1.7% for an ideal cosmic variance limited experiment. Constraints on α are of the order 0.3% for Planck and can in principle be as small as 0.1% using CMB data alone - tighter constraints will require further (non-CMB) priors.

I. INTRODUCTION

The recent release of the Wilkinson Microwave Anisotropy Probe (WMAP) first-year data [1, 2, 3, 4] has pushed cosmology into a new stage. On one hand, it has quantitatively validated the broad features of the ‘standard’ cosmological model—the optimistically called ‘concordance’ model. But at the same time, it has also pushed the borderline of research to new territory. We now know that ‘dark components’ make up the overwhelming majority of the energy budget of the universe. Most of this is almost certainly in some non-baryonic form, for which there is at present no direct evidence or solid theoretical explanation. One must therefore try to understand the nature of this dark energy, or at least (as

a first step) look for clues of its origin.

It is clear that such an effort must be firmly grounded within fundamental physics, and indeed that recent progress in fundamental physics may shed new light on this issue. On the other hand, this is not a one-way street. Cosmology and astrophysics are playing an increasingly more important role as fundamental physics testbeds, since they provide us with extreme conditions (that one has no hope of reproducing in terrestrial laboratories) in which to carry out a plethora of tests and search for new paradigms. Perhaps the more illuminating example is that of multidimensional cosmology. Currently preferred unification theories [5, 6] predict the existence of additional space-time dimensions, which will have a number of possibly observable consequences, including modifications in the gravitational laws on very large (or very small) scales [7] and space-time variations of the fundamental constants of nature [8, 9].

There have been a number of recent reports of evidence for a time variation of fundamental constants [10, 11, 12, 13], and apart from their obvious direct impact if confirmed they are also crucial in a different, indirect way. They provide us with an important (and possibly even unique) opportunity to test a number of fundamental physics models that might otherwise

*Electronic address: graca@mrao.cam.ac.uk

†Electronic address: roberto.trotta@physics.unige.ch

‡Electronic address: C.J.A.P.Martins@damtp.cam.ac.uk

§Electronic address: melch@astro.ox.ac.uk

¶Electronic address: ppavelin@fc.up.pt

**Electronic address: rbean@astro.princeton.edu

††Electronic address: viana@astro.up.pt

be untestable. A case in point is that of string theory [5]. Indeed here the issue is not *if* such a theory predicts such variations, but *at what level* it does so, and hence if there is any hope of detecting them in the near future (or if we have done it already). Indeed, it has been argued [6, 14] that even the results of Webb and collaborators [10, 11, 12] may be hard to explain in the simplest, best motivated models where the variation of alpha is driven by the spacetime variation of a very light scalar field. Playing devil's advocate, one could certainly conceive that cosmological observations of this kind could one day prove string theory wrong.

The most promising case, and the one that has been the subject of most recent work (and speculation), is that of the fine-structure constant α , for which some fairly strong statistical evidence of time variation at redshifts $z \sim 2-3$ already exists [10, 11, 12], together with weaker (and somewhat more controversial) evidence from geophysical tests using the Oklo natural nuclear reactor [15]. Interesting and quite tight constraints can also be derived from local laboratory tests [16], and indeed this is a context where improvements of several orders of magnitude can be expected in the coming years.

On the other hand, the theoretical expectation in the simplest, best motivated model is that α should be a non-decreasing function of time [17, 18, 19]. This is based on rather general and simple assumptions, in particular that the cosmological dynamics of the fine-structure constant is governed by a scalar field whose behavior is akin to that of a dilaton. If this is so, then it is particularly important to try to constrain it at earlier epochs, where any variations relative to the present-day value should therefore be larger. In this regard, note that one of the interpretations of the Oklo results [15] is that α was *larger* at the Oklo epoch (effectively $z \sim 0.1$) than today, whereas the quasar results [10, 11, 12] indicate that α was smaller at $z \sim 2-3$ than today. Both results are not necessarily incompatible, since they refer to two different cosmological epochs, and hence comparing them necessarily requires specifying not only a *background* cosmological model but also a model for the variation of the fine-structure constant with redshift, $\alpha = \alpha(z)$. However, if both results are validated by future experiments, then the above theoretical expectation must clearly be wrong (with clear implications for both the dilaton hypothesis and on a wider scale), which would be a perfect example of using astrophysics to learn about fundamental physics.

Cosmic microwave background (CMB) anisotropies provide an ideal way of measuring the fine-structure constant at high redshift, being mostly sensitive to the epoch of decoupling, $z \sim 1100$ (one could also envisage searching for spatial variations at the last scattering surface [20]). Here we continue our ongoing work in this area [21, 22, 23], and particularly extend our most recent analysis [24] of the WMAP first-year data, providing updated constraints on the value of α at decoupling, studying some crucial degeneracies with other cosmological parameters and discussing what improvements can be expected

with forthcoming datasets.

We emphasize that in previous (pre-WMAP) work, CMB-based constraints on α were obtained with the help of additional cosmological datasets and priors. This has raised some eyebrows among skeptics, as different datasets could possibly have different systematic errors that are impossible to control and could conceivably conspire to produce the results we quoted (statistically consistency with the value of α at decoupling being the same as today's, though with a slight preference towards smaller values). Here, by contrast, we will present results of an analysis of the WMAP dataset alone (we will only briefly discuss what happens when other datasets are added). We also discuss how these constraints can be improved in the future, especially when more precise CMB polarization data is available. In particular, we show that the existence of an early reionization epoch is a significant help in further constraining α , and indeed the prospects for measuring α from the CMB are much better than if the optical depth τ was much smaller.

Moreover, now that CMB polarization data is available, there are two approaches one can take. One is to treat CMB temperature and polarization as different datasets, and carry out independent analyses (and, more to the point, cosmological parameter estimations), to check if the results of the two are consistent. The other one is to combine the two datasets, thus getting smaller errors on the parameters. We will show that there are advantages to both approaches, and also that the combination of the two can often by itself break many of the cosmological degeneracies that plague this kind of analysis pipeline. On the other hand, we will also show that in ideal circumstances (*id est*, a cosmic variance limited experiment) CMB polarization is much better than CMB temperature in determining cosmological parameters. This result is not new, and it is of course somewhat obvious, but it has never been quantified in detail as will be done below.

On the other hand, because cosmic variance limited experiments are expensive and experimentalists work with limited budgets, it is important to provide detailed forecasts for future experiments. We provide detailed forecasts for the full (4-year) WMAP dataset, as well as for ESA's Planck Surveyor (to be launched in 2007). It will be shown that Planck is almost cosmic variance limited (taken into account the range of multipoles covered by this instrument) when it comes to CMB temperature, but far from it for CMB polarization. Again this was previously known, but had not been quantified. This, and the intrinsic superiority of CMB polarization in measuring cosmological parameters, are therefore arguments for a post-Planck, polarization-dedicated experiment.

II. CMB TEMPERATURE AND POLARIZATION

Following [25, 26, 27, 28], one can describe the CMB anisotropy field as a 2×2 , I_{ij} , intensity tensor which is a function of direction on the sky \hat{n} and 2 other directions perpendicular to \hat{n} which define its components \hat{e}_1, \hat{e}_2 . The CMB radiation is expected to be polarised due to Thomson scattering of temperature anisotropies at the time when CMB photons last scattered. Polarised light is traditionally described via the Stokes parameters, Q, U, V , where $Q = (I_{11} - I_{22})/4$ and $U = I_{12}/2$, while the temperature anisotropy is given by $T = (I_{11} + I_{22})/4$ and V can be ignored since it describes circular polarization which cannot be generated through Thomson scattering. Both Q and U depend of the choice of coordinate system in that they transform under a right handed rotation in the plane perpendicular to direction \hat{n} by an angle ψ as:

$$\begin{aligned} Q' &= Q \cos 2\psi + U \sin 2\psi \\ U' &= -Q \sin 2\psi + U \cos 2\psi, \end{aligned} \quad (1)$$

where $\hat{e}_1' = \cos \psi \hat{e}_1 + \sin \psi \hat{e}_2$ and $\hat{e}_2' = -\sin \psi \hat{e}_1 + \cos \psi \hat{e}_2$.

In order to compute the rotationally invariant power spectrum a general method to analyse polarization over the whole sky is required. This is so because the calculation of the power spectrum involves the superposition of the different modes contributing to the perturbations. While it is simple to compute Q and U in the coordinate system where the wavevector defining the perturbation is aligned with the z axis, it is more complicated to do so when superimposing the different modes since one needs to rotate Q and U to a common coordinate frame before this superposition is done, and only in the small scale limit does this rotation have a simple expression [29].

Most of the literature on the polarization of the CMB uses three alternative representations based on either the Newman-Penrose spin-weight 2 harmonics [25], or a coordinate representation of the tensor spherical harmonics [30, 31], or the coordinate-independent, projected symmetric trace free (PSTF) tensor valued multipoles [32]. Here we follow the first by expanding the polarization in the sky in terms of spin-weighted harmonics which form a basis for tensor functions in the sky. One starts by defining two other quantities $(Q \pm iU)'$:

$$(Q \pm iU)'(\hat{n}) = e^{\mp 2i\psi} (Q \pm iU)(\hat{n}). \quad (2)$$

These quantities are then expanded in the appropriate spin-weighted basis:

$$\begin{aligned} T(\hat{n}) &= \sum_{lm} a_{T,lm} Y_{lm}(\hat{n}) \\ (Q + iU)(\hat{n}) &= \sum_{lm} a_{2,lm} {}_2Y_{lm}(\hat{n}) \\ (Q - iU)(\hat{n}) &= \sum_{lm} a_{-2,lm} {}_{-2}Y_{lm}(\hat{n}), \end{aligned} \quad (3)$$

where Y_{lm} are the spherical harmonics and ${}_2Y_{lm}$ are the so-called spin-2 spherical harmonics, which form a complete and orthonormal basis for spin-2 functions. A function ${}_s f(\theta, \phi)$ defined on the sphere has spin- s if under a right-handed rotation of (\hat{e}_1, \hat{e}_2) by an angle ψ it transforms as ${}_s f'(\theta, \phi) = e^{-is\psi} {}_s f(\theta, \phi)$. Here we are interested in the polarization of the CMB which is a quantity of spin ± 2 .

Q and U are defined at a given direction \hat{n} with respect to the spherical coordinate system $(\hat{e}_\theta, \hat{e}_\phi)$. The expansion coefficients for the polarization variables satisfy $a_{-2,lm}^* = a_{2,l-m}$. For temperature the relation is $a_{T,lm}^* = a_{T,l-m}$, where

$$\begin{aligned} a_{T,lm} &= \int d\Omega Y_{lm}^*(\hat{n}) T(\hat{n}) \\ a_{2,lm} &= \int d\Omega {}_2Y_{lm}^*(\hat{n}) (Q + iU)(\hat{n}) \\ a_{-2,lm} &= \int d\Omega {}_{-2}Y_{lm}^*(\hat{n}) (Q - iU)(\hat{n}) \end{aligned} \quad (4)$$

Usually one considers the following linear combinations:

$$\begin{aligned} a_{E,lm} &= -(a_{2,lm} + a_{-2,lm})/2 \\ a_{B,lm} &= i(a_{2,lm} - a_{-2,lm})/2. \end{aligned} \quad (5)$$

The following rotationally invariant quantities then define the power spectra

$$\begin{aligned} C_{Tl} &= \frac{1}{2l+1} \sum_m \langle a_{T,lm}^* a_{T,lm} \rangle \\ C_{El} &= \frac{1}{2l+1} \sum_m \langle a_{E,lm}^* a_{E,lm} \rangle \\ C_{Bl} &= \frac{1}{2l+1} \sum_m \langle a_{B,lm}^* a_{B,lm} \rangle \\ C_{Cl} &= \frac{1}{2l+1} \sum_m \langle a_{T,lm}^* a_{E,lm} \rangle, \end{aligned} \quad (6)$$

in terms of which,

$$\begin{aligned} \langle a_{T,l'm'}^* a_{T,lm} \rangle &= C_{Tl} \delta_{l'l} \delta_{m'm} \\ \langle a_{E,l'm'}^* a_{E,lm} \rangle &= C_{El} \delta_{l'l} \delta_{m'm} \\ \langle a_{B,l'm'}^* a_{B,lm} \rangle &= C_{Bl} \delta_{l'l} \delta_{m'm} \\ \langle a_{T,l'm'}^* a_{E,lm} \rangle &= C_{Cl} \delta_{l'l} \delta_{m'm} \\ \langle a_{B,l'm'}^* a_{E,lm} \rangle &= \langle a_{B,l'm'}^* a_{T,lm} \rangle = 0. \end{aligned} \quad (7)$$

In real space one describes the polarization field in terms of two quantities that are scalars under rotation, E and B modes, defined as:

$$\begin{aligned} \tilde{E}(\hat{n}) &= \sum_{lm} \left[\frac{(l+2)!}{(l-2)!} \right]^{1/2} a_{E,lm} Y_{lm}(\hat{n}) \\ \tilde{B}(\hat{n}) &= \sum_{lm} \left[\frac{(l+2)!}{(l-2)!} \right]^{1/2} a_{B,lm} Y_{lm}(\hat{n}). \end{aligned} \quad (8)$$

These quantities are closely related to the rotationally invariant Laplacian of Q and U . In multipole space the relation is as follows

$$a_{(\bar{E},\bar{B}),lm} = \left[\frac{(l+2)!}{(l-2)!} \right]^{1/2} a_{(E,B),lm}. \quad (9)$$

While E remains unchanged under parity transformation, B changes its sign (similar to the behaviour of electric and magnetic fields). This decomposition is also useful because the B mode is a direct signature of the presence of a background of gravitational waves, since it cannot be produced by density fluctuations [25, 30]. Many models of inflation predict a significant gravity wave background. These tensor fluctuations generated during inflation have their largest effects on large angular scales and add in quadrature to the fluctuations generated by scalar modes. Whilst recent WMAP results placed limits on the amplitude of these tensor modes one still lacks an experimental evidence for the presence of a stochastic background of gravitational waves. As mentioned above the detection of the pseudo-scalar field B would provide invaluable information about Inflation in that they reflect the presence of such a background. Therefore to fully characterize the CMB anisotropies only four power spectra are needed—those for T, E, B and the cross-correlation between T and E . (Given that B has the opposite parity of E and T their cross-correlations with B vanishes.)

The first detection of polarization of the CMB was due to the DASI experiment [33], and more recently the WMAP experiment [3] has measured the TE cross-correlation power spectrum. An important result from these is the existence of reionization at larger redshifts than expected from the Gunn-Petterson through, an issue that we will discuss at length below.

III. THE CMB, α AND τ

The reason why the CMB is a good probe of variations of the fine-structure constant is that these alter the ionisation history of the universe [21, 34, 35, 36]. The dominant effect is a change in the redshift of recombination, due to a shift in the energy levels (and, in particular, the binding energy) of Hydrogen. The Thomson scattering cross-section is also changed for all particles, being proportional to α^2 . A smaller effect (which has so far been neglected) is expected to come from a change in the Helium abundance [37].

Increasing α increases the redshift of last-scattering, which corresponds to a smaller sound horizon. Since the position of the first Doppler peak (ℓ_{peak}) is inversely proportional to the sound horizon at last scattering, increasing α will produce a larger ℓ_{peak} [21]. This larger redshift of last scattering also has the additional effect of producing a larger early ISW effect, and hence a larger amplitude of the first Doppler peak [34, 35]. Finally, an increase in α decreases the high- ℓ diffusion damping

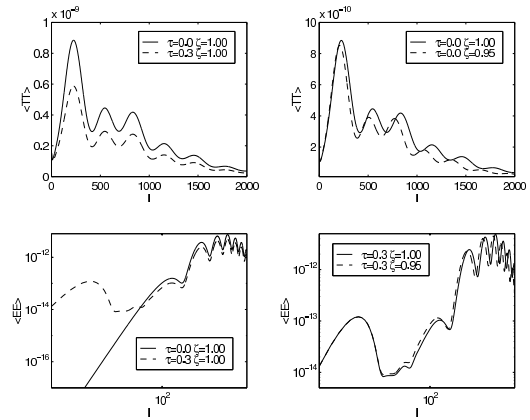


FIG. 1: Contrasting the effects of varying α (right) and reionization (left) on the CMB temperature (top) and polarization (bottom). Here $\zeta = \alpha_{dec}/\alpha_0$. See the text for further details.

(which is essentially due to the finite thickness of the last-scattering surface), and thus increases the power on very small scales. These effects have been implemented in a modified CMBFAST algorithm which allows a varying α parameter [21, 22]. These follow the extensive description given in [34, 35], with one important exception that will be discussed below.

Fig. 1 illustrates the effect of α and τ on the CMB temperature and polarization power spectra. The CMB power spectrum is, to a good approximation, insensitive to *how* α varies from last scattering to today. Given the existing observational constraints, one can therefore calculate the effect of a varying α in both the temperature and polarization power spectra by simply assuming two values for α , one at low redshift (effectively today's value, since any variation of the magnitude of [10] would have no noticeable effect) and one around the epoch of decoupling, which may be different from today's value. (In earlier works [21, 34, 35, 38] one assumed a constant value of α throughout, *id est* the values at reionization and the present day were always the same.)

For the CMB temperature, reionization simply changes the amplitude of the acoustic peaks, without affecting their position and spacing (top left panel); a different value of α at the last scattering, on the other hand, changes both the amplitude and the position of the peaks (top right panel).

The outstanding effect of reionization is to introduce a bump in the polarization spectrum at large angular scales (lower left panel). This bump is produced well after decoupling (at much lower redshifts), when α , if varying, is much closer to the present day's value. If the value of α

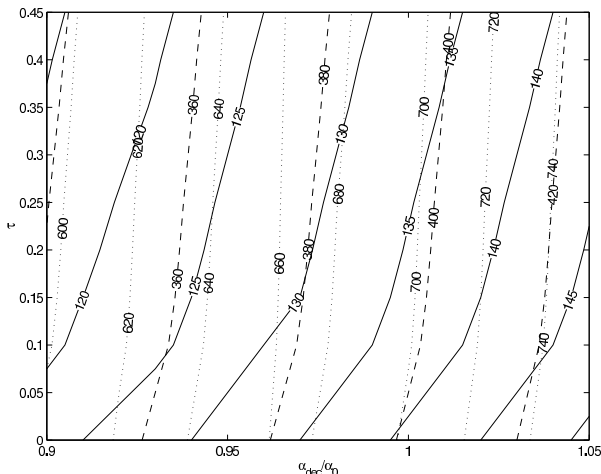


FIG. 2: The separation in ℓ between the reionization bump and the first (solid lines), second (dashed) and third (dotted) peaks in the polarization spectrum, as a function of α at decoupling and τ . A (somewhat idealized) description of how α and τ can be measured using CMB polarization.

at low redshift is different from that at decoupling, the peaks in the polarization power spectrum at small angular scales will be shifted sideways, while the reionization bump on large angular scales won't (lower right panel). It follows that by measuring the separation between the normal peaks and the bump, one can measure both α and τ , as illustrated in Fig. 2. Thus we expect that the existence of an early reionization epoch will, when more accurate cosmic microwave background polarization data is available, lead to considerably tighter constraints on α .

A possible concern with the interpretation of our results is related to the implicit assumption of a sharp transition on the value of α happening sometime between recombination and the epoch of reionization. Hence, it is crucial to understand if this is a valid approximation. Apart from the value of α at the time of recombination the knowledge of its value at two other epochs is relevant as far as the CMB anisotropies are concerned. One such epoch is the period *just before* recombination which is very important for the damping of CMB anisotropies on small angular scales. The other period is the epoch of reionization. In this work we effectively assume that α is equal to α_{rec} before recombination and to α_0 at the reionization epoch.

A value of α different from α_0 at the epoch of reionization will affect the CMB anisotropies through a change in the optical depth τ , *once a single cosmological model*

is assumed. However, it is also well known that τ is itself dependent on the cosmological model through its cosmological parameters (Ω_m and Ω_Λ for example) as well as on the cosmological density perturbations (in our case through the initial power spectrum) [39]. The exact dependence is difficult to determine since there are several astrophysical uncertainties related to a number of relevant non-linear physical processes which affect the accuracy of reionization models. In general, this problem is solved by treating τ as a free parameter (independent of the other cosmological parameters and initial power spectrum), which accounts for the relatively poor knowledge of the dependence of τ on the cosmological model and in our case on the uncertainty about the exact value of α during the reionization epoch. Hence, we find that provided we treat τ as a free parameter the lack of a precise knowledge of value of α during the epoch of reionization will not affect our results. In the present work, we assume that the universe was completely reionized in a relatively small redshift interval (sudden reionization). A more refined modelling of the reionization history is not yet required by WMAP data, but will be necessary at noise levels appropriate for Planck and beyond [40, 41, 42, 43]. On the more practical side, there are of course observational constraints on the value of α at redshifts of a few [10, 11, 12], indicating that at that epoch the possible changes relative to the present day are already very small (and would not be detectable, on their own, through the CMB due to cosmic variance).

The knowledge of the value of α before recombination is also crucial for the details of the damping of small scale CMB anisotropies. Let's assume that the variation of α around the time of recombination is given by some functional, f :

$$\frac{\alpha}{\alpha_{rec}} = f\left(\frac{1+z}{1+z_{rec}}\right)$$

One can determine the dependence of the Silk damping scale [44]

$$R_S = \left(\int_0^{t_{dec}(\alpha)} dt \frac{\lambda_\gamma(\alpha)}{R^2(t)}\right)^{\frac{1}{2}}$$

(where, λ_γ , is the photon mean free path) on this functional f and determine α_{eff} (relevant for the damping of CMB anisotropies) as the constant value of α that gives the same Silk damping scale as the variable one. Even though we did not treat α_{eff} as another parameter in the present investigation (this will be done in future work) we expect that our constraints on α_{rec} should also be valid (to a good approximation) for α_{eff} . This means that we are already able to constrain a combination of both α and f at the time of recombination. Also, we see that we may be able to rule out particular models for the time variation of α on the basis of the details of such variation, even if the value of α at the time of recombination is not ruled out by our analysis.

Finally, we must emphasize that the effects discussed above are direct effects of an α variation, and that indirect effects are usually present as well since any variation of α is necessarily coupled with the dynamics of the Universe [45]. In this paper we take a pragmatic approach and say that, since the CMB is quite insensitive to the details of α variations from decoupling to the present day, *we do not in fact need to specify a redshift dependence for this variation*—although we could have specified one if we so chose.

The price to pay would be that, since this coupling is very dependent on the particular model we consider we would end up with very model-dependent constraints. Therefore, at this stage, and given the lack of detailed and well-motivated cosmological models for α variations we prefer to focus on model-independent constraints, and hence do not attempt to include this extra degree of freedom in our analysis. Nevertheless, given some model-independent constraints one can always translate them into constraints on the parameters of one's favourite model. In fact we expect that some models will be ruled out on the basis of the indirect effect of a variation of α on the dynamics of the Universe rather than the direct effects we described above. This is actually a simpler case in which only the modifications to the background evolution ($a(t)$) would need to be taken into account in order to test the model, with the direct effects of a varying α being negligible.

We conclude this section by emphasising that although a more detailed analysis taking into account the expected variation of α with time (and its direct and indirect implications for CMB anisotropies) for specific models is certainly possible, our more general work can easily be used to impose very strong constraints to more complex varying α theories once the relevant variables are computed.

IV. UP-TO-DATE CMB CONSTRAINTS ON α WITH WMAP

We compare the recent WMAP temperature and cross-polarization dataset with a set of flat cosmological models adopting the likelihood estimator method described in [4]. We restrict the analysis to flat universes. The models are computed through a modified version of the CMBFAST code with parameters sampled as follows: physical density in cold dark matter $0.05 < \Omega_c h^2 < 0.20$ (step 0.01), physical density in baryons $0.010 < \Omega_b h^2 < 0.028$ (step 0.001), $0.500 < \Omega_\Lambda < 0.950$ (step 0.025), $0.900 < \alpha_{\text{dec}}/\alpha_0 < 1.050$ (step 0.005). Here h is the Hubble parameter today, $H_0 \equiv 100h \text{ km s}^{-1} \text{ Mpc}^{-1}$ (determined by the flatness condition once the above parameters are fixed), while α_{dec} (α_0) is the value of the fine structure constant at decoupling (today). We also vary the optical depth τ in the range $0.06 - 0.30$ (step 0.02), the scalar spectral index of primordial fluctuations $0.880 < n_s < 1.08$ (step 0.005) and its running

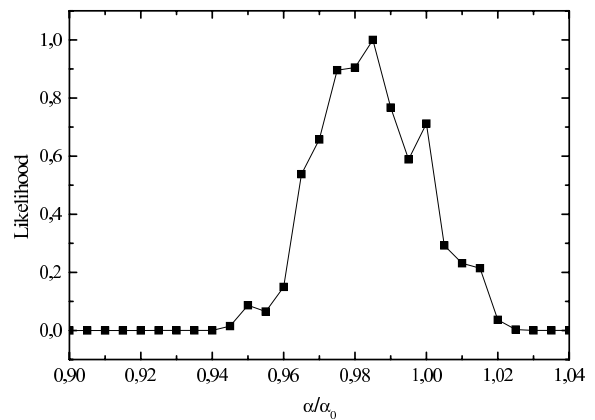


FIG. 3: Likelihood distribution function for variations in the fine structure constant obtained by an analysis of the WMAP data (TT+TE, one-year).

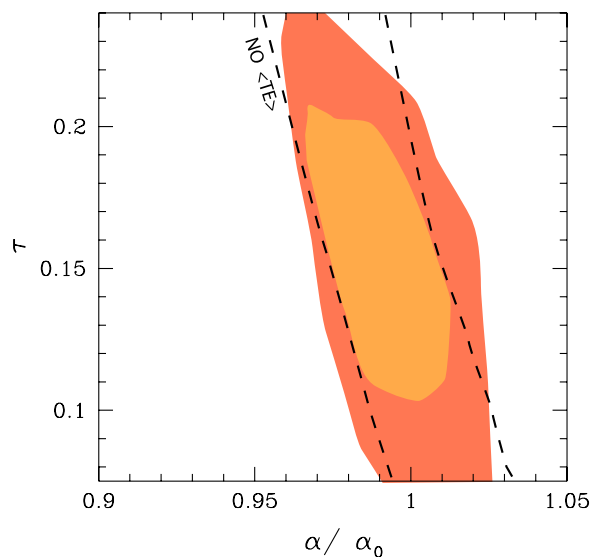


FIG. 4: 2-D Likelihood contour plot in the α/α_0 vs τ plane for 2 analysis: $\langle TT \rangle$ only and $\langle TT \rangle + \langle TE \rangle$. As we can see, the inclusion of polarization data, breaks the degeneracy between these 2 parameters.

$-0.15 < dn_s/dlnk < 0.05$ (step 0.01) both evaluated at $k_0 = 0.002 \text{ Mpc}^{-1}$. We don't consider gravity waves or iso-curvature modes since these further modifications are not required by the WMAP data (see e.g. [46]). A different model for the dark energy from a cosmological constant could also change our results, but again, is not suggested by the WMAP data (see e.g. [47]). An extra background of relativistic particles is also well constrained by Big Bang Nucleosynthesis (see e.g. [48]) and it will not be considered here.

The likelihood distribution function for $\alpha_{\text{dec}}/\alpha_0$, obtained after marginalization over the remaining parameters, is plotted in Figure 3. We found, at 95% C.L. that $0.95 < \alpha_{\text{dec}}/\alpha_0 < 1.02$, improving previous bounds, (see [23]) based on CMB and complementary datasets.

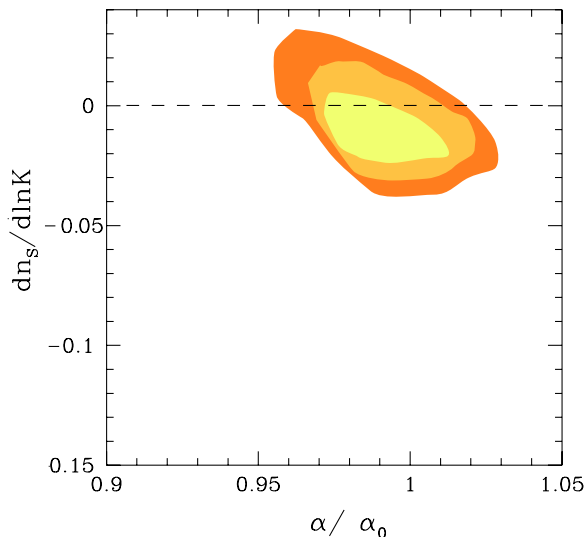


FIG. 5: 2-D Likelihood contour plot in the α/α_0 vs $dn_S/d\ln k$ plane ($\langle TT \rangle + \langle TE \rangle$ one year). A zero scale dependence, as expected in most of the inflationary models, is more consistent with a value of $\alpha/\alpha_0 < 1$

Setting $dn_S/d\ln k = 0$, yields $0.94 < \alpha_{\text{dec}}/\alpha_0 < 1.01$ as already reported in (see [24]).

It is interesting to consider the correlations between a α/α_0 and the other parameters in order to see how this modification to the standard model can change our conclusions about cosmology.

In Figure 4 we plot the 2-D likelihood contours in the α/α_0 vs the optical depth τ for 2 different analysis: using the temperature only WMAP data and including the $\langle TE \rangle$ cross spectrum temperature-polarization data. As we can see, there is a clear degeneracy between these 2 parameters if one consider just the $\langle TT \rangle$ spectrum: increasing the optical depth, allows for an higher value of the spectral index n_S and a lower value of α/α_0 (again, see [23]). As we can see from Figure 4, the inclusion of the $\langle TE \rangle$ data, is already able to partially break the degeneracy between τ and α/α_0 . However, as we explain below, more detailed measurements of the polarization spectra are needed to fully break this degeneracy.

One of the most unexpected results from the WMAP data is the hint for a scale-dependence of the spectral index n_S (see e.g. [49], [50]). Such dependence is not predicted to be detectable in most of the viable single field inflationary model and, if confirmed, will therefore have strong consequences on the possibilities of reconstructing the inflationary potential. In Figure 5 we plot a 2-D likelihood contour in the α/α_0 vs $dn_S/d\ln k$ plane. As we can see, a lower value of α/α_0 makes a value of $dn_S/d\ln k \sim 0$ more compatible with the data. As already noticed in [51], a modification of the recombination scheme can therefore provide a possible explanation for the high value of $dn_S/d\ln k$ compatible with the WMAP data.

V. FISHER MATRIX ANALYSIS SETUP

In our previous work [23], a Fisher Matrix Analysis was carried out, using only the CMB temperature, in order to estimate the precision with which cosmological parameters can be reconstructed in future experiments. Here we extend this analysis by including also E-polarization measurements as well as the TE cross-correlation. We consider the planned Planck satellite (HFI only) and an ideal experiment which would measure both temperature and polarization to the cosmic variance limit (in the following, 'CVL experiment') for a range of multipoles, l , up to 2000. For illustration purposes, and particularly as a way of checking that our method is producing credible results, we will also present the FMA analysis for WMAP, and compare the corresponding 'predictions' with existing results.

The Fisher Matrix is a measure of the width and shape of the likelihood around its maximum and as such can also provide useful insight into the degeneracies among different parameters, with minimal computational effort. For a review of this technique, see [52, 53, 54, 55, 56, 57, 58, 59, 60]. In what follows we will present a brief description of our analysis procedure, emphasizing the aspects that are new. We refer the reader to our previous work [23] for further details.

We will assume that cosmological models are characterized by the 8 dimensional parameter set

$$\Theta = (\Omega_b h^2, \Omega_m h^2, \Omega_\Lambda h^2, \mathcal{R}, n_s, Q, \tau, \alpha), \quad (10)$$

where $\Omega_m = \Omega_c + \Omega_b$ is the energy density in matter, Ω_Λ the energy density due to a cosmological constant, and h is a dependent variable which denotes the Hubble parameter today, $H_0 \equiv 100h \text{ km s}^{-1} \text{ Mpc}^{-1}$. The quantity $\mathcal{R} \equiv \ell_{\text{ref}}/\ell$ is the 'shift' parameter (see [61, 62] and references therein), which gives the position of the acoustic peaks with respect to a flat, $\Omega_\Lambda = 0$ reference model. The shift parameter \mathcal{R} depends on Ω_m , on the curvature $\Omega_\kappa \equiv 1 - \Omega_\Lambda - \Omega_m - \Omega_{\text{rad}}$ through

$$\mathcal{R} = 2 \left(1 - \frac{1}{\sqrt{1 + z_{\text{dec}}}} \right) \times \frac{\sqrt{|\Omega_\kappa|}}{\Omega_m} \frac{1}{\chi(y)} \left[\sqrt{\Omega_{\text{rad}} + \frac{\Omega_m}{1 + z_{\text{dec}}}} - \sqrt{\Omega_{\text{rad}}} \right] \quad (11)$$

where z_{dec} is the redshift of decoupling, Ω_{rad} is the energy parameter due to radiation ($\Omega_{\text{rad}} = 4.13 \cdot 10^{-5}/h^2$ for photons and 3 neutrinos) and

$$y = \sqrt{|\Omega_\kappa|} \int_0^{z_{\text{dec}}} dz \quad (12)$$

$$[\Omega_{\text{rad}}(1+z)^4 + \Omega_m(1+z)^3 + \Omega_\kappa(1+z)^2 + \Omega_\Lambda]^{-1/2}.$$

The function $\chi(y)$ depends on the curvature of the universe and is y , $\sin(y)$ or $\sinh(y)$ for flat, closed or open models, respectively. Inclusion of the shift parameter \mathcal{R}

TABLE I: Experimental parameters for WMAP and Planck (nominal mission). Note that we express the sensitivities in μK .

	WMAP			Planck		
ν (GHz)	40	60	90	100	143	217
θ_c (arcmin)	31.8	21.0	13.8	10.7	8.0	5.5
$\sigma_c T$ (μK)	19.8	30.0	45.6	5.4	6.0	13.1
σ_{cE} (μK)	28.02	42.43	64.56	n/a	11.4	26.7
$w_c^{-1} \cdot 10^{15}$ ($\text{K}^2 \text{ster}$)	33.6	33.6	33.6	0.215	0.158	0.350
ℓ_c	254	385	586	757	1012	1472
ℓ_{max}	1000			2000		
f_{sky}	0.80			0.80		

into our set of parameters takes into account the geometrical degeneracy between ω_Λ and ω_m [59]. With our choice of the parameter set, \mathcal{R} is an independent variable, while the Hubble parameter h becomes a dependent one.

n_s is the scalar spectral index and $Q = \langle \ell(\ell+1)C_\ell \rangle^{1/2}$ denotes the overall normalization, where the mean is taken over the multipole range $2 \leq \ell \leq 2000$.

We assume purely adiabatic initial conditions and we do not allow for a tensor contribution. In the FM approach, the likelihood distribution \mathcal{L} for the parameters Θ is expanded to quadratic order around its maximum \mathcal{L}_m . We denote this maximum likelihood (ML) point by Θ_0 and call the corresponding model our “ML model”, with parameters $\omega_b = 0.0200$, $\omega_m = 0.1310$, $\omega_\Lambda = 0.2957$ (and $h = 0.65$), $\mathcal{R} = 0.9815$, $n_s = 1.00$, $Q = 1.00$, $\tau = 0.20$ and $\alpha/\alpha_0 = 1.00$. For the value of z_{dec} (which is weakly dependent on ω_b and ω_{tot}) we have used the fitting formula from [63]. For the ML model we have $z_{\text{dec}} = 1115.52$.

As mentioned above we also present the FMA for the WMAP best fit model as the fiducial model. (ie, $\omega_b = 0.0200$, $\omega_m = 0.1267$, $\omega_\Lambda = 0.2957$, $\mathcal{R} = 0.9636$, $n_s = 0.99$, $Q = 1.00$, $\tau = 0.17$ and $\alpha/\alpha_0 = 1.00$.) Note that we will discuss cases with and without reionization (in the latter case $\tau = 0.0$) as well as with and without varying α .

To compute the derivatives of the power spectrum with respect to a particular cosmological parameter one varies the considered parameter and keeps fixed the value of the others to their ML value. In particular given that we are not constraining our analysis to the case of a flat universe a variation in \mathcal{R} is considered with all the other parameters fixed and equal to their ML value. Therefore such variation implies a variation of the dependent parameter h .

In our previous work [23] we assumed a flat fiducial model, and differentiating around it requires computing open and closed models, which are calculated using different numerical techniques. We have found that this can limit the accuracy of the FMA. Here we instead differentiate around a slightly closed model (as preferred

by WMAP) with $\Omega_{\text{tot}} = 1.01$ to avoid extra sources of numerical inaccuracies. We refer to [23] for a detailed description of the numerical technique used. The experimental parameters used for the Planck analysis are in Table I. Note that we use the first 3 channels of the Planck High Frequency Instrument (HFI) only. Adding the 3 channels of Planck’s Low Frequency Instrument leaves the expected errors unchanged: therefore they can be used for other important tasks such as foreground removal and various consistency checks, leaving the HFI channels for direct cosmological use. For the CVL experiment, we set the experimental noise to zero, and we use a total sky coverage $f_{\text{sky}} = 1.00$. Although this is never to be achieved in practice, the CVL experiment illustrates the precision which can be obtained *in principle* from CMB temperature and E-polarization measurements.

If the errors $\Theta - \Theta_0$ about the ML model are small, a quadratic expansion around this ML leads to the expression,

$$\mathcal{L} \approx \mathcal{L}_m \exp \left[-\frac{1}{2} \sum_{ij} F_{ij} \delta\Theta_i \delta\Theta_j \right] \quad (13)$$

where F_{ij} is the Fisher matrix, given by derivatives of the CMB power spectrum with respect to the parameters Θ

In [23] we computed the *Fisher information matrix* using temperature information alone. In this case for each l a derivative of the temperature power spectrum with respect to the parameter under consideration is computed and then summed over all l , weighted by $Cov^{-1}(\hat{C}_{Tl}^2) = \Delta C_\ell^2$, that is

$$F_{ij} = \sum_{\ell=2}^{\ell_{\text{max}}} \frac{1}{\Delta C_\ell^2} \frac{\partial C_\ell}{\partial \Theta_i} \frac{\partial C_\ell}{\partial \Theta_j} \Big|_{\Theta_0}. \quad (14)$$

The quantity ΔC_ℓ is the standard deviation on the estimate of C_ℓ :

$$\Delta C_\ell^2 = \frac{2}{(2\ell+1)f_{\text{sky}}} (C_\ell + B_\ell^{-2})^2; \quad (15)$$

the first term is the cosmic variance, arising from the fact that we exchange an ensemble average with a spatial average. The second term takes into account the expected error of the experimental apparatus [56, 59],

$$B_\ell^2 = \sum_c w_c e^{-\ell(\ell+1)/\ell_c^2}. \quad (16)$$

The sum runs over all channels of the experiment, with the inverse weight per solid angle $w_c^{-1} \equiv (\sigma_c \theta_c)^{-2}$ and $\ell_c \equiv \sqrt{8 \ln 2} / \theta_c$, where σ_c is the sensitivity (expressed in μK) and θ_c is the FWHM of the beam (assuming a Gaussian profile) for each channel. Furthermore, we can neglect the issues arising from point sources, foreground removal and galactic plane contamination assuming that once they have been taken into account we are left with a “clean” fraction of the sky given by f_{sky} .

In the more general case with polarization information included, instead of a single derivative we have a vector of four derivatives with the weighting given by the inverse of the covariance matrix [25],

$$F_{ij} = \sum_l \sum_{X,Y} \frac{\partial \hat{C}_{Xl}}{\partial \Theta_i} \text{Cov}^{-1}(\hat{C}_{Xl} \hat{C}_{Yl}) \frac{\partial \hat{C}_{Yl}}{\partial \Theta_j}, \quad (17)$$

where F_{ij} is the Fisher information or curvature matrix as above, Cov^{-1} is the inverse of the covariance matrix, Θ_i are the cosmological parameters we want to estimate and X, Y stands for T (temperature), E, B (polarization modes), or C (cross-correlation of the power spectra for T and E). For each l one has to invert the covariance matrix and sum over X and Y . The diagonal terms of the covariance matrix between the different estimators are given by

$$\begin{aligned} \text{Cov}(\hat{C}_{Tl}^2) &= \frac{2}{(2\ell+1)f_{\text{sky}}} (\hat{C}_{Tl} + B_{T\ell}^{-2})^2 \\ \text{Cov}(\hat{C}_{El}^2) &= \frac{2}{(2\ell+1)f_{\text{sky}}} (\hat{C}_{El} + B_{P\ell}^{-2})^2 \\ \text{Cov}(\hat{C}_{Cl}^2) &= \frac{1}{(2\ell+1)f_{\text{sky}}} \left[\hat{C}_{Cl}^2 + (\hat{C}_{Tl} + B_{T\ell}^{-2})(\hat{C}_{El} + B_{P\ell}^{-2}) \right] \\ \text{Cov}(\hat{C}_{Bl}^2) &= \frac{2}{(2\ell+1)f_{\text{sky}}} (\hat{C}_{Bl} + B_{P\ell}^{-2})^2. \end{aligned} \quad (18)$$

The non-zero off diagonal terms are

$$\begin{aligned} \text{Cov}(\hat{C}_{Tl} \hat{C}_{El}) &= \frac{2}{(2\ell+1)f_{\text{sky}}} \hat{C}_{Cl}^2 \\ \text{Cov}(\hat{C}_{Tl} \hat{C}_{Cl}) &= \frac{2}{(2\ell+1)f_{\text{sky}}} \hat{C}_{Cl} (\hat{C}_{Tl} + B_{T\ell}^{-2}) \\ \text{Cov}(\hat{C}_{El} \hat{C}_{Cl}) &= \frac{2}{(2\ell+1)f_{\text{sky}}} \hat{C}_{Cl} (\hat{C}_{El} + B_{P\ell}^{-2}), \end{aligned} \quad (19)$$

where $B_{T\ell}^{-2} = B_{\ell}^{-2}$ as above and $B_{P\ell}^{-2}$ is obtained using a similar expression but with the experimental specifications for the polarized channels.

For Gaussian fluctuations, the covariance matrix is then given by the inverse of the Fisher matrix, $C = F^{-1}$ [58]. The 1σ error on the parameter Θ_i with all other parameters marginalised is then given by $\sqrt{C_{ii}}$. If all other parameters are held fixed to their ML values, the standard deviation on parameter Θ_i reduces to $\sqrt{1/F_{ii}}$ (conditional value). Other cases, in which some of the parameters are held fixed and others are being marginalised over can easily be worked out.

In the case in which all parameters are being estimated jointly, the joint error on parameter i is given by the projection on the i -th coordinate axis of the multi-dimensional hyper-ellipse which contains a fraction γ of the joint likelihood. The equation of the hyper-ellipse is

$$(\Theta - \Theta_0) \mathbf{F} (\Theta - \Theta_0)^t = q_{1-\gamma}, \quad (20)$$

where $q_{1-\gamma}$ is the quantile for the probability $1 - \gamma$ for a χ^2 distribution with 6,7 and 8 degrees of freedom. For

$\gamma = 0.683$ (1σ c.l.) we have for 6,7 and 8 degrees of freedom, $q_{1-\gamma} = 7.03$, $q_{1-\gamma} = 8.18$ and $q_{1-\gamma} = 9.30$, respectively.

As observed in [23] the accuracy with which parameters can be determined depends on their true value as well as on the number of parameters considered. Note that the FMA *assumes* that the values of the parameters of the true model are in the vicinity of Θ_0 . The validity of the results therefore depends on this assumption, as well as on the assumption that the $a_{\ell m}$'s are independent Gaussian random variables. If the FMA predicted errors are small enough, the method is self-consistent and we can expect the FMA prediction to reproduce in a correct way the exact behaviour. This is indeed the case for the present analysis, with the notable exception of ω_Λ , which as expected suffers from the geometrical degeneracy.

Also, special care must be taken when computing the derivatives of the power spectrum with respect to the cosmological parameters. This differentiation strongly amplifies any numerical errors in the spectra, leading to larger derivatives, which would artificially break degeneracies among parameters. In the present work we implement double-sided derivatives, which reduce the truncation error from second order to third order terms. The choice of the step size is a trade-off between truncation error and numerical inaccuracy dominated cases. For an estimated numerical precision of the computed models of order 10^{-4} , the step size should be approximately 5% of the parameter value [64], though it turns out that for derivatives in direction of α and n_s the step size can be chosen to be as small as 0.1%. After several tests, we have chosen step sizes varying from 1% to 5% for $\omega_b, \omega_m, \omega_\Lambda$ and \mathcal{R} . This choice gives derivatives with an accuracy of about 0.5%. The derivatives with respect to Q are exact, being the power spectrum itself.

VI. FMA WITHOUT REIONIZATION

We will now start to describe the results of our analysis in detail. In order to avoid confusion, we will begin in this chapter by describing the results for the case $\tau = 0$ (since most of the crucial degeneracies can be understood in this case), and leave the more relevant case of non-zero τ for the following chapter. While it may seem pointless after WMAP to discuss the cases without (or with very little) reionization, we shall see that a lot can be learned by comparing the results for the various cases.

A. Analysis results: The FMA forecast

Tables II–V summarize the results of our FMA for WMAP, Planck and a CVL experiment. We consider the cases of models with and without a varying α being included in the analysis, for $\tau = 0$. We also consider the use of temperature information alone (TT), E-polarization alone (EE) and both channels (EE+TT) jointly.

TABLE II: Fisher matrix analysis results for Standard model: expected 1σ errors for the WMAP and Planck satellites as well as for a CVL experiment. The column *marg.* gives the error with all other parameters being marginalized over; in the column *fixed* the other parameters are held fixed at their ML value; in the column *joint* all parameters are being estimated jointly.

Quantity	1σ errors (%)								
	WMAP			Planck HFI			CVL		
	marg.	fixed	joint	marg.	fixed	joint	marg.	fixed	joint
	Polarization								
ω_b	1437.41	52.93	4111.09	6.40	0.99	18.31	0.48	0.25	1.38
ω_m	619.43	31.47	1771.62	3.57	0.33	10.22	0.70	0.03	2.01
ω_Λ	1397.45	980.08	3996.79	38.76	34.40	110.84	11.28	9.94	32.27
n_s	260.43	33.68	744.83	1.47	0.91	4.20	0.30	0.08	0.86
Q	474.57	25.13	1357.31	2.21	0.45	6.32	0.24	0.07	0.68
\mathcal{R}	666.04	22.10	1904.92	3.53	0.30	10.09	0.66	0.03	1.88
	Temperature								
ω_b	2.79	1.26	7.97	0.82	0.59	2.36	0.55	0.38	1.59
ω_m	4.58	0.83	13.11	1.44	0.12	4.12	1.09	0.08	3.11
ω_Λ	115.59	86.53	330.59	91.65	86.37	262.11	80.68	77.25	230.74
n_s	1.50	0.52	4.30	0.48	0.13	1.36	0.33	0.07	0.96
Q	0.80	0.34	2.29	0.19	0.10	0.55	0.17	0.07	0.48
\mathcal{R}	4.17	0.73	11.92	1.41	0.11	4.03	1.05	0.07	2.99
	Temperature and Polarization								
ω_b	2.78	1.26	7.95	0.77	0.51	2.20	0.32	0.21	0.91
ω_m	4.56	0.83	13.05	1.16	0.12	3.32	0.55	0.03	1.58
ω_Λ	114.34	86.09	327.03	31.79	31.72	90.92	9.87	9.49	28.24
n_s	1.50	0.52	4.28	0.39	0.13	1.12	0.20	0.06	0.57
Q	0.80	0.34	2.28	0.18	0.10	0.52	0.14	0.05	0.40
\mathcal{R}	4.15	0.73	11.86	1.14	0.10	3.25	0.52	0.03	1.49

Table II shows the 1σ errors on each of the parameters of our FMA for a ‘standard model’, that is with no reionization or variation of α . The inclusion of polarization data does indeed increase the accuracy on each parameter for Planck and for a CVL experiment. For the Planck mission the polarization data helps to better constrain each of the parameters though the increase in accuracy is only of the order 10% in most cases. The error in ω_Λ is still large, and larger than those of the other parameters. Indeed, this error is almost insensitive to the experimental details when only temperature is considered in the analysis, which of course is a manifestation of the so-called geometrical degeneracy [59, 60].

The existence of this nearly exact degeneracy limits in a fundamental way the accuracy on measurements of the Hubble constant as well as of the curvature of the universe obtained with the CMB observations, and hence limits the accuracy on ω_m and ω_Λ . This degeneracy can only be removed when constraints on the geometry of the universe from other complementary observations, such as Type Ia supernova or gravitational lensing, are jointly considered [59, 60]. Our plots show that actually using polarization data the confidence contours can narrow significantly on the ω_Λ axis. This case is very different from other degeneracies between parameters which actu-

ally can be broken with good enough CMB data and by probing a larger set of angular scales ie an enlarged range of multipoles l , as well as using the CMB polarised data.

The geometrical degeneracy gives rise to almost identical CMB anisotropies in universes with different background geometries but identical matter content, lines of constant \mathcal{R} are directions of degeneracy. This degeneracy along $\delta(\omega_m^{-1/2}\mathcal{R}) = 0$ results in a linear relation between $\delta\omega_k$ and $\delta\omega_\Lambda$, with coefficients that depend on the fiducial model.

This is why we used the \mathcal{R} parameter to replace ω_k in our fisher analysis instead of the ω_D parameter of [59, 60].

The accuracy on the parameter \mathcal{R} is related to the ability of fixing the positions of the Doppler peaks. Hence Planck is expected to determine \mathcal{R} with high accuracy given that it samples the Doppler peak region almost entirely. Indeed this is the case with the error reducing from 4% for WMAP to 1% for Planck and to 0.5% for a CVL experiment (see Table II).

Table III shows the 1σ errors on each of the parameters of our FMA for a model with a time-varying α . While the inclusion of a varying α as a parameter (with the nominal value equal to that of the standard model) has no noticeable effect on the accuracy of the other parameters for a CVL experiment, for Planck and most notoriously

TABLE III: Fisher matrix analysis results for a model with a varying α : expected 1σ errors for the WMAP and Planck satellites as well as for a CVL experiment. The column *marg.* gives the error with all other parameters being marginalized over; in the column *fixed* the other parameters are held fixed at their ML value; in the column *joint* all parameters are being estimated jointly.

Quantity	1σ errors (%)								
	WMAP			Planck HFI			CVL		
	marg.	fixed	joint	marg.	fixed	joint	marg.	fixed	joint
	Polarization								
ω_b	4109.93	52.93	11754.68	6.42	0.99	18.36	1.10	0.25	3.16
ω_m	844.65	31.47	2415.75	7.14	0.33	20.43	1.64	0.03	4.69
ω_Λ	1483.80	980.08	4243.77	41.78	34.40	119.50	12.03	9.94	34.41
n_s	365.06	33.68	1044.09	3.90	0.91	11.16	0.79	0.08	2.25
Q	2415.47	25.13	6908.40	3.24	0.45	9.28	0.24	0.07	0.69
\mathcal{R}	4847.40	22.10	13863.91	10.13	0.30	28.98	1.19	0.03	3.39
α	887.24	3.51	2537.58	2.62	0.05	7.50	0.40	< 0.01	1.15
	Temperature								
ω_b	10.41	1.26	29.78	0.97	0.59	2.78	0.77	0.38	2.21
ω_m	8.51	0.83	24.34	2.54	0.12	7.27	2.04	0.08	5.85
ω_Λ	125.00	86.53	357.51	107.64	86.37	307.85	93.06	77.25	266.16
n_s	3.05	0.52	8.73	1.32	0.13	3.76	1.04	0.07	2.97
Q	2.11	0.34	6.05	0.20	0.10	0.57	0.17	0.07	0.50
\mathcal{R}	21.12	0.73	60.40	1.50	0.11	4.29	1.06	0.07	3.02
α	4.64	0.12	13.27	0.43	0.02	1.22	0.31	0.01	0.88
	Temperature and Polarization								
ω_b	10.00	1.26	28.60	0.87	0.51	2.49	0.38	0.21	1.09
ω_m	8.23	0.83	23.54	1.61	0.12	4.60	0.67	0.03	1.90
ω_Λ	123.13	86.09	352.17	31.79	31.72	90.92	9.96	9.49	28.49
n_s	2.97	0.52	8.48	0.85	0.13	2.44	0.32	0.06	0.91
Q	2.04	0.34	5.82	0.18	0.10	0.53	0.14	0.05	0.41
\mathcal{R}	20.34	0.73	58.18	1.36	0.10	3.88	0.60	0.03	1.72
α	4.46	0.12	12.75	0.31	0.02	0.88	0.11	< 0.01	0.32

for WMAP this is not the case (compare Table II with Table III). For these two satellite missions the accuracy of most of the other parameters is reduced by inclusion of this extra parameter as should be expected (for allowing an extra degree of freedom). The same trend as before is observed with the inclusion of polarization data.

From our WMAP predictions one would expect to be able to constrain α to about 5% accuracy at 1σ while the actual analysis presented in previous section gives an accuracy of the order of 7% at 2σ . This is in reasonable agreement with our prediction with the discrepancy being due to the effect of a $\tau \neq 0$ (see next section). On the other hand, the results of our forecast are that Planck and a CVL experiment will be able to constrain variations in α with an accuracy of 0.3% and 0.1% respectively (1σ c.l., all other parameters marginalized). If all parameters are being estimated simultaneously, then these limits increase to about 0.9% and 0.3% respectively. This is therefore the best that one can hope to do with the CMB alone—it is somewhat below the 10^{-5} level of the claimed detection of a variation using quasar absorp-

tion systems [10, 11, 12], but it is also at a much higher redshift, where any variations relative to the present day are expected to be larger than at $z \sim 3$. Therefore, for specific models such limits can be at least as constraining as those at low redshift. On the other hand, there *is* a way of doing better than this, which is to combine CMB data with other observables—this is the approach we already took in [22, 23], for example.

From these tables we conclude that for WMAP the inclusion of polarization information does not improve significantly the accuracy on each of the parameters, since its accuracy from polarization data alone is expected to be worse than that from temperature alone by a factor of $\simeq 10^2 - 10^3$. With Planck though there is room for improvement, with the accuracy from polarization alone at most only a factor 10 poorer than from temperature. Also for this case a better accuracy on ω_Λ is obtained using polarization data alone vs using temperature data alone, for both cases with and without inclusion of a varying α . For the CVL experiment the polarization makes a real difference, with the accuracy of polarization alone

being *slightly better* than that of the temperature alone. Combining the two typically increases the accuracy on most parameters by a factor of order 2. As expected this is most noticeably so for ω_Λ . Assuming that the improvement was only owing to the use of independent sets of data we should expect an improvement by at least a factor of $\sqrt{2}$.

B. Analysis results: Confidence contours

In order to provide better intuition for the various effects involved, we show in Figs. 6-7 joint 2D confidence contours for all pairs of parameters (all remaining parameters marginalized) for the cases shown in Tables II-III respectively (that is, the cases $\tau = 0$ without and with a varying α). For each case we show plots corresponding to our three experiments (WMAP, Planck and CVL), and contours for TT only, EE only and all combined. Note that all contours are 2σ . To notice that in the WMAP case the errors from E only are very large, hence the contours for T coincide almost exactly with the temperature-polarization combined case. In the CVL case it is the E contours that almost coincide with the combined ones.

Again, starting with the standard model in Fig. 6 we can observe the expected degeneracies between parameters, as previously discussed in [59, 60]. These degeneracies among parameters limit our ability to disentangle one parameter from another, using CMB observations alone. The search for means to break such degeneracies is therefore of extreme importance.

The contour plots for WMAP exhibit the degeneracy directions in the planes $(\omega_\Lambda, \mathcal{R})$, (n_s, \mathcal{R}) , for example \mathcal{R} suffers strong degeneracy with ω_m , ω_Λ . A correlation between ω_Λ and both n_s and Q is also noticeable. The contour plot in the plane $(\omega_\Lambda, \mathcal{R})$ prevents a good constraint of both parameters in agreement with results tabulated in Table II. For both Planck and a CVL experiment the direction of degeneracy for polarization alone is almost orthogonal to this direction while the direction for temperature alone corresponds to $\mathcal{R} = \text{constant}$. The degeneracy direction on the (ω_m, \mathcal{R}) plane is defined by $\delta(\omega_m^{1/2}\mathcal{R})=0$.

The contour plots for Planck are perhaps the perfect example of a case where the degeneracy directions between \mathcal{R} and ω_Λ are different and almost orthogonal for Temperature and Polarization alone. This therefore explains why the joint use of T and E data helps to break degeneracies. For example the degeneracy between \mathcal{R} and ω_b present when polarization is considered alone, disappears when temperature information is included. It is interesting to notice, when comparing WMAP and Planck plots, that the joint use of T and E does not necessarily break degeneracies between the parameters, whilst narrowing down the width of the contour plots without affecting the degeneracy directions.

For the CVL experiment the effect of polarization is to better constrain all parameters in particular ω_Λ , help-

ing to narrow down the range of allowed values in the ω_Λ direction as compared with Temperature alone. For instance in the plane (n_s, ω_Λ) the direction n_s is well constrained but there is no discriminatory power on the ω_Λ direction until polarization data is included. For all but the 2D planes containing ω_Λ , the contours are narrowed to give better constraints to each of the parameters. This is due to the exact degeneracy mentioned above: more accurate CMB measurements simply narrow the likelihood contours around the degeneracy lines on the $(\omega_\Lambda, \omega_k)$ plane [59, 60].

Fig. 6 also shows that ω_b and ω_m are slightly anti-correlated for the Planck experiment. For the WMAP experiment the plot shows a degeneracy between ω_m and ω_Λ . If we restrict ourselves to spatially flat models there is a relationship between these two parameters that will result in similar position of the Doppler peaks. The degeneracy direction can be obtained by differentiating l_D , the location of the maximum of the first Doppler peak [59, 60] These degeneracy lines in the $\omega_c - \omega_\Lambda$ plane are given by (assuming that ω_b is held fixed in the expression of l_D):

$$\omega_c = (\omega_c)_t + b\omega_\Lambda; b = -\frac{(\partial l_D / \partial \omega_\Lambda)_t}{(\partial l_D / \partial \omega_c)_t} \quad (21)$$

Unlike the geometrical degeneracy, this is not exact. Both the height and the amplitude of the peaks depend upon the parameter ω_m , hence an experiment such as Planck which probes high multipoles will be able to break this degeneracy. This is clearly visible in Fig. 6 for both Planck and a CVL experiment (compare with the case for WMAP).

Similarly the condition of constant height of the first Doppler peak determines the degeneracies among ω_b , ω_c , n_s and Q . Both WMAP and Planck are sensitive to higher multipoles than the first Doppler peak. The other peaks help to pin down the value of ω_b and therefore these degeneracies can actually be broken. The plots for WMAP show a mild degeneracy in the (n_s, ω_b) plane for the EE+TT+ET joint analysis, which seems to be lifted for the Planck experiment.

In our previous works [21, 22, 23] we observed a degeneracy between α and some of the other parameters, most notably ω_b , n_s and \mathcal{R} . Our previous FMA analysis with temperature information alone [23] showed that these degeneracies could be removed by using higher multipole measurements, e.g., from Planck. The question we want to address here is whether the use of polarization data allows further improvements.

As previously pointed out, a variation in α affects both the location and height of the Doppler peaks, hence this parameter will be correlated with parameters that determine the peak structure. Therefore, from the previous discussion on degeneracies among parameters for a standard model, one can anticipate the degeneracies exhibited in Fig. 7 in the planes (α, n_s) , (α, \mathcal{R}) , (α, Q) , (α, ω_b) and (α, ω_m) .

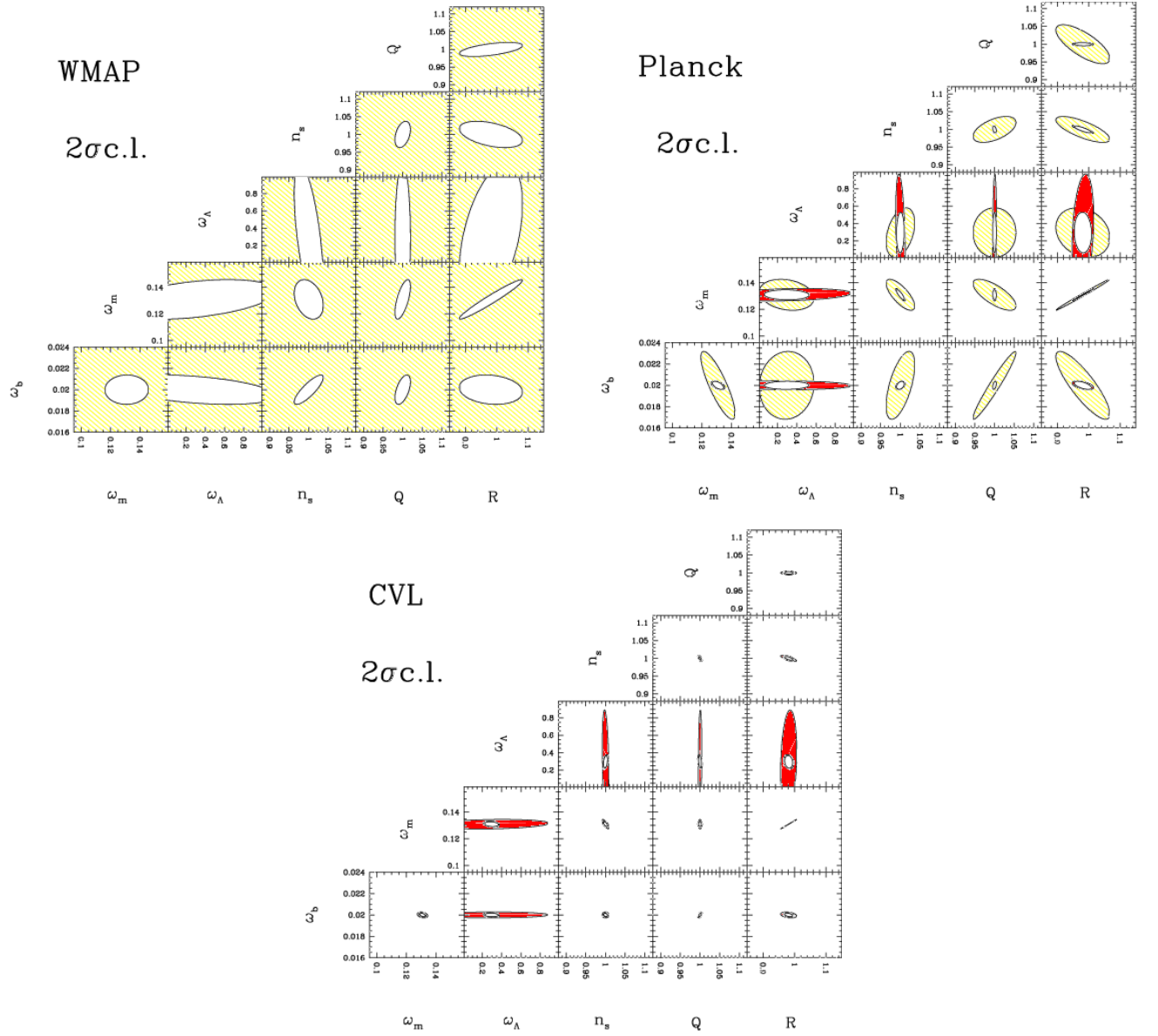


FIG. 6: Ellipses containing 95.4% (2σ) of joint confidence (all other parameters marginalized) using temperature alone (red), E-polarization alone (yellow), and both jointly (white), for a standard model. In the WMAP case the errors from E only are very large, hence the contours for T coincide almost exactly with the temperature-polarization combined case. In the CVL case it is the E contours that almost coincide with the combined ones.

In our previous work [23] we showed that using temperature alone the degeneracies of α with ω_b and α with n_s are lifted as we move from WMAP to Planck when higher multipoles measurements can break it.

All the degeneracy directions for these pairs of parameters for the WMAP joint analysis (which actually is dominated by the temperature data alone) are approximately preserved by using polarization data alone for the Planck experiment. A joint analysis of temperature and polarization helps to narrow down the confidence contours without necessarily breaking the degeneracy.

With the inclusion of the new parameter α the WMAP

contour plots get wider as compared with Fig. 6, while leaving almost unchanged the degeneracy directions in most planes of pairs of parameters. For Planck the contour plots are still wider whilst the degeneracy directions for polarization alone change for some of the parameters. For example, the direction of degeneracy between the (\mathcal{R}, n_s) changes when compared with Fig. 6, which is due to the presence of the degeneracy between α and n_s which is almost orthogonal to the direction of degeneracy in the plane (α, ω_m) . Another changed direction of degeneracy is that of (ω_b, \mathcal{R}) , with wider contour plots. The degeneracy present in the WMAP plot for the plane

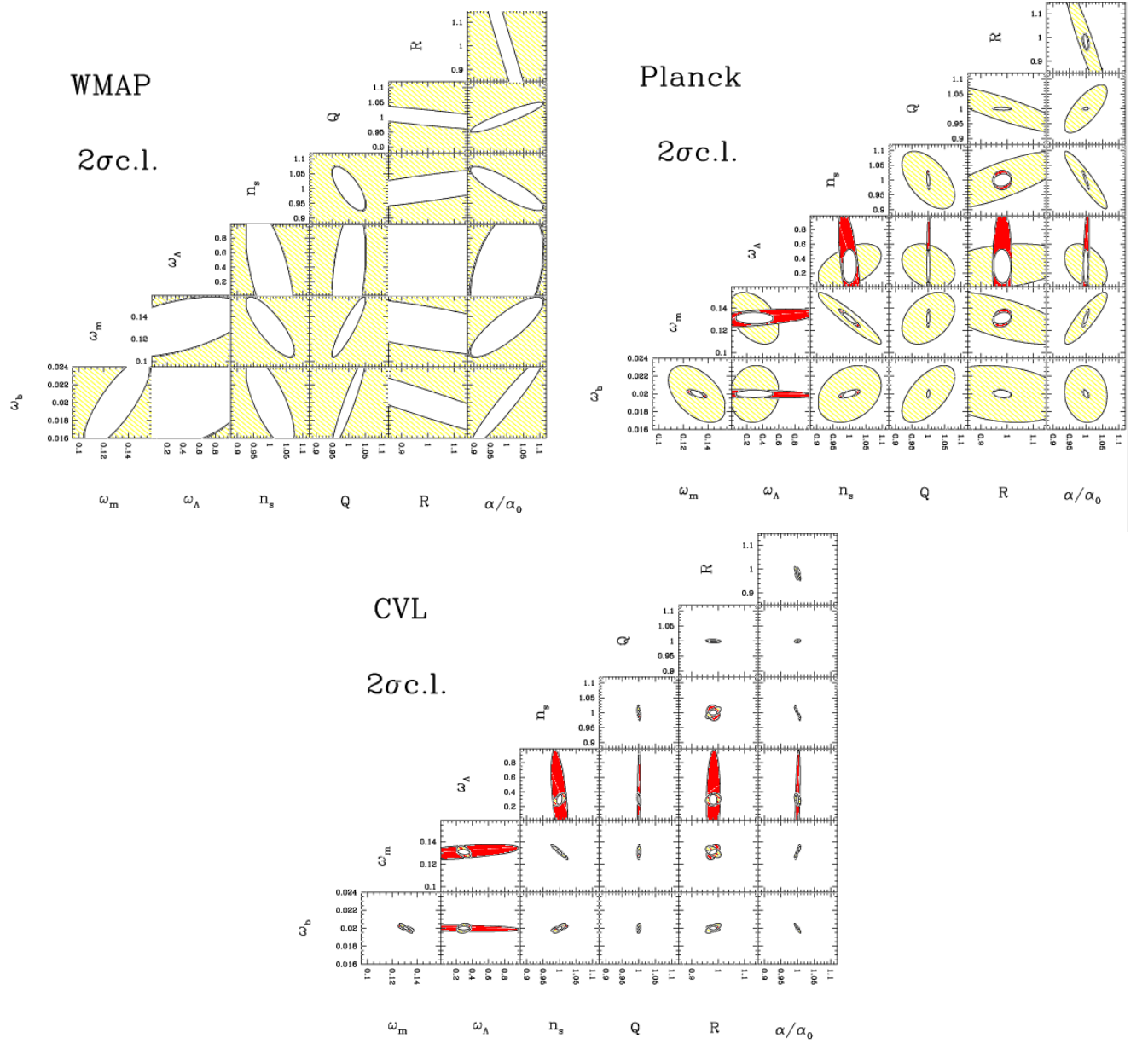


FIG. 7: Ellipses containing 95.4% (2σ) of joint confidence (all other parameters marginalized) using temperature alone (red), E-polarization alone (yellow), and both jointly (white), for a model with varying α . In the WMAP case the errors from E only are very large, hence the contours for T coincide almost exactly with the temperature-polarization combined case. In the CVL case it is the E contours that almost coincide with the combined ones.

(α, ω_b) seems to be broken with Planck data. Notice the strong degeneracy between α and \mathcal{R} which still persists when using jointly temperature and polarization data.

Using Temperature and Polarization data jointly seems either to help to break some of the degeneracies or at least to narrow down the contours without lifting the degeneracy, in particular for those cases where the degeneracy directions for each of the temperature and polarization are different (in some cases almost orthogonal see for example the planes containing ω_Λ as one of the parameters).

For the CVL experiment most of the plots remain un-

changed when compared with no inclusion of α , with the temperature alone contour plot slightly wider in the (n_s, ω_Λ) plane. A large range of possibilities along the ω_Λ direction still remains as expected from the exact geometrical degeneracy mentioned above.

C. Analysis results: Principal directions

The power of an experiment can be roughly quantified by looking at the eigenvalues λ_i and eigenvectors $\mathbf{u}^{(i)}$ of

TABLE IV: For a model with a varying α and the case Temperature and Polarization considered jointly. In the lines we display the components of the eigenvectors of the FM for WMAP, Planck and a CVL experiment. The quantity $1/\sqrt{\lambda_i}$ is proportional to the error along the principal direction $\mathbf{u}^{(i)}$. For each principal direction, an asterisk marks the largest cosmological parameters contribution, a dagger the second largest. Not only Planck has errors smaller by a factor of about 5 on average, but also the alignment of the principal directions with the axis defined by the physical parameter is better than WMAP in 6 cases out of 7.

WMAP								
Direction i	$1/\sqrt{\lambda_i}$	ω_b	ω_m	ω_Λ	n_s	Q	\mathcal{R}	α
1	2.50E-04	9.9446E-01*	-9.9203E-02†	-2.5224E-05	-2.7487E-02	-3.9411E-03	1.2295E-02	1.6954E-02
2	8.84E-04	8.1778E-02	7.0553E-01*	-5.6359E-04	-6.8131E-02	2.4777E-02	-1.1338E-01	-6.9096E-01†
3	2.24E-03	4.8801E-02	5.2913E-01 †	9.3752E-04	2.6766E-01	-6.3566E-01*	4.0924E-02	4.9016E-01
4	1.24E-02	4.2341E-02	2.5947E-01	1.2292E-02	6.5656E-01†	6.6964E-01*	4.5581E-02	2.2174E-01
5	1.48E-02	1.0147E-02	3.7938E-01	-3.5290E-02	-6.9349E-01*	3.7432E-01	2.0829E-01	4.3623E-01†
6	1.94E-01	-9.0774E-03	-2.9295E-02	2.2193E-01†	8.9661E-02	-7.8874E-02	9.4671E-01*	-1.9819E-01
7	3.71E-01	1.9270E-03	1.7036E-02	9.7435E-01*	-5.4121E-02	2.3700E-02	-2.0877E-01†	5.7273E-02
Planck								
Direction i	$1/\sqrt{\lambda_i}$	ω_b	ω_m	ω_Λ	n_s	Q	\mathcal{R}	α
1	9.02E-05	7.9666E-01*	-4.4311E-01†	-1.2864E-05	4.6149E-03	-1.4650E-02	6.7622E-02	4.0518E-01
2	1.38E-04	6.0235E-01*	5.7873E-01†	1.1892E-05	-3.3913E-02	-5.8211E-02	-8.4462E-02	-5.3905E-01
3	4.80E-04	2.5914E-02	6.1004E-01†	-1.5285E-05	3.4825E-01	3.4725E-01	2.8006E-02	6.2011E-01*
4	1.88E-03	4.0978E-02	-2.0888E-01	2.2619E-04	-7.9733E-02	9.3426E-01*	2.5167E-03	-2.7474E-01†
5	8.88E-03	1.2289E-02	-2.2979E-01	-3.4989E-03	9.1281E-01*	-4.7146E-02	-2.2075E-01	-2.5072E-01†
6	1.36E-02	-1.1477E-03	1.1923E-02	7.0929E-03	1.9486E-01†	-2.7260E-02	9.6887E-01*	-1.4961E-01
7	9.40E-02	4.5352E-05	-8.4463E-04	9.9997E-01*	1.8356E-03	-1.7712E-04	-7.6431E-03†	2.6714E-04
CVL								
Direction i	$1/\sqrt{\lambda_i}$	ω_b	ω_m	ω_Λ	n_s	Q	\mathcal{R}	α
1	2.67E-05	-1.2198E-01	7.5184E-01*	1.6953E-05	-4.5292E-03	-1.5331E-03	-1.0829E-01	-6.3883E-01†
2	4.30E-05	9.8787E-01*	1.5297E-01†	-4.0577E-06	2.3058E-02	-2.0123E-03	-1.1111E-02	-6.8706E-03
3	2.26E-04	-8.5658E-02	5.3126E-01†	-1.6190E-04	3.8153E-01	4.0338E-01	2.5197E-02	6.3365E-01*
4	1.30E-03	4.2889E-02	-2.9019E-01	4.2863E-03	6.5704E-02	8.8528E-01*	1.3375E-02	-3.5457E-01†
5	3.31E-03	7.1120E-03	-2.0415E-01	-3.3636E-02	9.1855E-01*	-2.2722E-01	-8.6918E-02	-2.3286E-01†
6	5.95E-03	-2.8965E-05	5.6352E-02	1.1741E-02	7.0270E-02	-4.2538E-02	9.8973E-01*	-1.0183E-01†
7	2.95E-02	4.7963E-05	-6.2146E-03	9.9936E-01*	2.9871E-02†	-1.0880E-02	-1.4605E-02	-5.0067E-03

its FM: The error along the direction in parameter space defined by $\mathbf{u}^{(i)}$ (principal direction) is proportional to $\lambda_i^{-1/2}$. It can be measured by assessing how the principal components mix inflationary variables (such as n_s) with physical cosmic densities. The accuracy on the former is typically limited by cosmic variance (the derivatives of C_l with respect to these variables has large amplitude for low multipoles; the accuracy on the latter is set by the accuracy with which the C_l is measured at high multipoles (the derivatives of the angular power spectrum with respect to these variables is larger for $l \sim 2000 - 3000$).

But we are interested in determining the errors on the physical parameters rather than on their linear combinations along the principal directions. Therefore in the ideal case we want the principal directions to be as much aligned as possible to the coordinate system defined by the physical parameters. We display in Table IV eigenvalues and eigenvectors of the FM for WMAP and Planck and a CVL experiment. Planck's errors, as measured by

the inverse square root of the eigenvalues, are smaller by a factor of about 6 on average than those for WMAP (to be compared with a factor of 4 using temperature alone obtained in our previous analysis [23]) While a CVL experiment's errors are smaller by a factor of about 3 on average than those for Planck.

For 5 of the 7 eigenvectors Planck also obtains a better alignment of the principal directions with the axis of the physical parameters. This is established by comparing the ratios between the largest (marked with an asterisk in Tables IV) and the second largest (marked with a dagger) cosmological parameters' contribution to the principal directions. This is of course in a slightly different form the statement that Planck will measure the cosmological parameters with less correlations among them. It is to be noticed that for Planck direction 7 is mostly aligned with ω_Λ . While α is the second largest parameter contribution to two of the principal directions for both WMAP and Planck, this is the case for four principal directions

TABLE V: For a model with a varying α and the case (TT) ie Temperature only. In the lines we display the components of the eigenvectors of the FM for WMAP, Planck and a CVL experiment. The quantity $1/\sqrt{\lambda_i}$ is proportional to the error along the principal direction $\mathbf{u}^{(i)}$. For each principal direction, an asterisk marks the largest cosmological parameters contribution, a dagger the second largest. Not only Planck has errors smaller by a factor of about 4 on average, but also the alignment of the principal directions with the axis defined by the physical parameter is better than WMAP in 6 cases out of 7.

WMAP								
Direction i	$1/\sqrt{\lambda_i}$	ω_b	ω_m	ω_Λ	n_s	Q	\mathcal{R}	α
1	2.50E-04	9.9447E-01*	-9.9159E-02†	-2.5230E-05	-2.7515E-02	-3.9234E-03	1.2276E-02	1.6802E-02
2	8.84E-04	8.1646E-02	7.0565E-01*	-5.6626E-04	-6.8099E-02	2.4756E-02	-1.1338E-01	-6.9086E-01†
3	2.24E-03	4.8844E-02	5.2886E-01†	9.4022E-04	2.6766E-01	-6.3596E-01*	4.0937E-02	4.9006E-01
4	1.24E-02	4.2256E-02	2.5530E-01	1.2657E-02	6.6444E-01†	6.6515E-01*	4.4102E-02	2.1685E-01
5	1.49E-02	1.0648E-02	3.8232E-01	-3.5272E-02	-6.8593E-01*	3.8154E-01	2.0973E-01	4.3865E-01†
6	2.00E-01	-9.0958E-03	-2.9575E-02	2.3865E-01†	8.8766E-02	-7.9309E-02	9.4276E-01*	-1.9779E-01
7	3.78E-01	2.0990E-03	1.7737E-02	9.7038E-01*	-5.5730E-02	2.5328E-02	-2.2492E-01†	6.0883E-02
Planck								
Direction i	$1/\sqrt{\lambda_i}$	ω_b	ω_m	ω_Λ	n_s	Q	\mathcal{R}	α
1	1.01E-04	7.2972E-01*	-5.0661E-01†	1.3138E-06	6.7011E-03	-6.9279E-03	7.5433E-02	4.5284E-01
2	1.54E-04	6.8066E-01*	5.0680E-01	-1.8992E-05	-4.2986E-02	-6.6152E-02	-7.8097E-02	-5.1724E-01†
3	4.94E-04	5.4883E-02	6.2059E-01*	2.1300E-05	3.4975E-01	3.5572E-01	2.4796E-02	6.0198E-01†
4	1.95E-03	3.3117E-02	-2.1287E-01	-8.9072E-04	-9.9243E-02	9.3131E-01*	3.4607E-03	-2.7638E-01†
5	1.14E-02	9.3798E-03	-2.3387E-01	2.6011E-02	9.2519E-01*	-3.5345E-02	-1.1636E-01	-2.7161E-01†
6	1.49E-02	-2.3014E-03	3.6400E-02	2.0129E-03	9.6754E-02	-2.1077E-02	9.8694E-01*	-1.2173E-01†
7	3.18E-01	-1.9911E-04	5.8193E-03	9.9966E-01*	-2.4365E-02†	1.7831E-03	1.0413E-03	7.0427E-03
CVL								
Direction i	$1/\sqrt{\lambda_i}$	ω_b	ω_m	ω_Λ	n_s	Q	\mathcal{R}	α
1	5.86E-05	6.7177E-01*	-4.8930E-01	8.7005E-07	3.9437E-02	2.7795E-02	8.1011E-02	5.4811E-01†
2	1.16E-04	7.3379E-01*	5.3949E-01†	-1.2978E-05	-2.8027E-05	-2.4037E-02	-7.2166E-02	-4.0585E-01
3	2.91E-04	-9.4755E-02	6.0914E-01†	1.7574E-05	3.4556E-01	3.4843E-01	1.1703E-02	6.1564E-01*
4	1.71E-03	3.4674E-02	-2.0806E-01	-8.4424E-04	-8.2888E-02	9.3517E-01*	1.4441E-02	-2.7182E-01†
5	9.14E-03	9.1126E-03	-1.9125E-01	2.0128E-02	8.9154E-01*	-5.1488E-02	2.8905E-01†	-2.8615E-01
6	1.05E-02	-3.6709E-03	1.3640E-01	-9.7678E-03	-2.7727E-01†	-7.0379E-03	9.5096E-01*	6.0169E-03
7	2.75E-01	-1.7944E-04	5.0041E-03	9.9975E-01*	-2.0734E-02†	1.7511E-03	3.4827E-03	5.5738E-03

for a CVL experiment, and is also the largest parameter contribution to two and one of the principal directions for Planck and a CVL experiment respectively.

For comparison we also display in Table V eigenvalues and eigenvectors of the FM for WMAP and Planck and a CVL experiment using Temperature information alone. Comparing Tables IV and V we conclude that for WMAP the largest and second largest parameter contribution to the principal direction are exactly the same. On the other hand for Planck 2 of the principal directions change namely direction 7, whose main contribution is from ω_Λ and n_s when Temperature information alone is used while when Polarization is included the second largest contribution comes now from \mathcal{R} . For direction 3 the largest and second largest contribution are interchanged (arising from ω_m and α) when polarization is included. Finally for a CVL experiment for direction 1 the second largest contribution from α is replaced by ω_m when polarization is included. For direction 2 both

largest contribution change from ω_b to ω_m and that from ω_m (second largest) to α . The major contributions for the remaining directions remain the same while the second largest contribution changes for all of them. Only for 2 and 3 of the 7 eigenvectors Planck and a CVL experiment respectively obtain a better alignment of the principal directions with the axis of the physical parameters (with the other directions equally aligned), when polarization is included.

Therefore we conclude that indeed polarization does not necessarily help to further break degeneracies between parameters when no information on reionization or tensor component of the CMB is included.

VII. FMA WITH REIONIZATION

The existence of a period when the intergalactic medium was reionized as well as its driving mechanism

TABLE VI: Fisher matrix analysis results for a standard model with inclusion of reionization ($\tau = 0.20$): expected 1σ errors for the WMAP and Planck satellites as well as for a CVL experiment. The column *marg.* gives the error with all other parameters being marginalized over; in the column *fixed* the other parameters are held fixed at their ML value; in the column *joint* all parameters are being estimated jointly.

Quantity	1σ errors (%)								
	WMAP			Planck HFI			CVL		
	marg.	fixed	joint	marg.	fixed	joint	marg.	fixed	joint
	Polarization								
ω_b	223.67	22.18	639.70	6.21	1.11	17.75	0.48	0.25	1.38
ω_m	104.48	22.12	298.81	3.37	0.39	9.64	0.70	0.03	1.99
ω_Λ	1231.56	113.78	3522.35	37.37	22.87	106.89	11.40	9.99	32.61
n_s	107.77	5.31	308.22	1.53	0.96	4.38	0.30	0.08	0.86
Q	139.04	18.38	397.68	2.23	0.51	6.38	0.24	0.07	0.67
\mathcal{R}	91.43	20.44	261.50	3.33	0.35	9.52	0.65	0.03	1.86
τ	156.71	9.64	448.22	5.74	2.78	16.42	1.81	1.52	5.18
	Temperature								
ω_b	10.59	1.35	30.28	0.86	0.60	2.46	0.57	0.38	1.64
ω_m	13.54	0.88	38.72	1.51	0.13	4.31	1.10	0.08	3.14
ω_Λ	114.06	96.36	326.22	110.15	96.15	315.03	98.15	86.00	280.72
n_s	8.64	0.53	24.72	0.54	0.13	1.56	0.36	0.07	1.04
Q	1.46	0.36	4.19	0.20	0.11	0.56	0.17	0.07	0.50
\mathcal{R}	13.98	0.78	39.98	1.47	0.12	4.21	1.05	0.07	3.01
τ	107.58	13.26	307.68	16.50	8.28	47.20	14.02	5.89	40.09
	Temperature and Polarization								
ω_b	3.10	1.34	8.86	0.80	0.53	2.30	0.32	0.21	0.92
ω_m	5.09	0.88	14.56	1.24	0.12	3.55	0.55	0.03	1.58
ω_Λ	89.62	72.75	256.33	30.58	22.04	87.46	10.72	9.85	30.65
n_s	1.66	0.52	4.76	0.43	0.13	1.23	0.20	0.05	0.58
Q	0.96	0.36	2.74	0.19	0.10	0.53	0.14	0.05	0.41
\mathcal{R}	4.49	0.78	12.85	1.22	0.11	3.48	0.52	0.03	1.49
τ	12.38	7.90	35.41	4.04	2.65	11.56	1.73	1.48	4.96

are still to be understood. One possible way of studying this phase is via the CMB polarization anisotropy. The optical depth to electrons of the CMB photons enhances the polarization signal at large angular scales (see Fig. 1) introducing a bump in the polarization spectrum at small multipoles. On the other hand reionization decreases the amplitude of the acoustic peaks on the temperature power spectrum at intermediate and small angular scales. This signal has now been detected by WMAP via the temperature polarization cross power-spectrum [3].

In the absence of polarization observations, the optical depth to Thomson scattering is degenerate with the amplitude of the fluctuations, Q (with $Qe^\tau = \text{constant}$). From previous Fisher Matrix Analysis for a standard model, e.g. [57], one expects that the inclusion of polarization measurements will help to better constrain some of the cosmological parameters, by probing the ionization history of the universe, hence constraining τ and breaking degeneracies of this with other parameters. We will now repeat the analysis of the previous chapter for the

case $\tau \neq 0$.

A. Analysis results: The FMA forecast

Tables VI–XI summarize the results of our FMA for WMAP, Planck and a CVL experiment. We consider the cases of models with and without a varying α being included in the analysis, and also two values of the optical depth, $\tau = 0.2$ (close to the one preferred by WMAP) and $\tau = 0.02$. We also consider the use of temperature information alone (TT), E-polarization alone (EE) and both channels (EE+TT) jointly. To show that our FMA fiducial model is close enough to the WMAP best fit model to produce similar FMA results, we display in Table XII the results of our FMA using as fiducial model the WMAP best fit model.

For the sake of completeness we also consider the case (TE) alone as well as (EE+TE) and (EE+TT+TE) for WMAP 4-years. Table XIV display the results of

TABLE VII: Fisher matrix analysis results for a model with varying α and inclusion of reionization ($\tau = 0.20$): expected 1σ errors for the WMAP and Planck satellites as well as for a CVL experiment. The column *marg.* gives the error with all other parameters being marginalized over; in the column *fixed* the other parameters are held fixed at their ML value; in the column *joint* all parameters are being estimated jointly.

Quantity	1σ errors (%)								
	WMAP			Planck HFI			CVL		
	marg.	fixed	joint	marg.	fixed	joint	marg.	fixed	joint
	Polarization								
ω_b	281.91	22.18	806.27	6.46	1.11	18.47	1.09	0.25	3.12
ω_m	446.89	22.12	1278.15	7.75	0.39	22.17	1.61	0.03	4.60
ω_Λ	1248.94	113.78	3572.04	41.61	22.87	119.01	11.60	9.99	33.17
n_s	126.90	5.31	362.93	4.14	0.96	11.85	0.77	0.08	2.22
Q	200.97	18.38	574.78	2.99	0.51	8.55	0.24	0.07	0.68
\mathcal{R}	254.76	20.44	728.63	9.56	0.35	27.33	1.19	0.03	3.40
α	111.52	3.74	318.96	2.66	0.06	7.62	0.40	< 0.01	1.14
τ	275.13	9.64	786.88	8.81	2.78	25.19	2.26	1.52	6.45
	Temperature								
ω_b	13.56	1.35	38.78	1.09	0.60	3.12	0.83	0.38	2.37
ω_m	17.73	0.88	50.71	3.76	0.13	10.74	2.64	0.08	7.55
ω_Λ	137.68	96.36	393.77	111.61	96.15	319.21	98.97	86.00	283.05
n_s	10.10	0.53	28.88	2.18	0.13	6.24	1.49	0.07	4.26
Q	2.41	0.36	6.89	0.20	0.11	0.57	0.18	0.07	0.50
\mathcal{R}	23.86	0.78	68.25	1.58	0.12	4.53	1.06	0.07	3.04
α	5.16	0.13	14.76	0.66	0.02	1.88	0.41	0.01	1.18
τ	111.97	13.26	320.24	26.93	8.28	77.02	20.32	5.89	58.11
	Temperature and Polarization								
ω_b	7.37	1.34	21.07	0.91	0.53	2.61	0.38	0.21	1.09
ω_m	6.94	0.88	19.85	1.81	0.12	5.17	0.67	0.03	1.91
ω_Λ	89.69	72.75	256.51	30.89	22.04	88.36	10.79	9.85	30.85
n_s	2.32	0.52	6.65	0.97	0.13	2.77	0.33	0.05	0.93
Q	1.63	0.36	4.67	0.19	0.10	0.54	0.14	0.05	0.41
\mathcal{R}	14.22	0.78	40.68	1.43	0.11	4.08	0.60	0.03	1.72
α	3.03	0.13	8.68	0.34	0.02	0.97	0.11	< 0.01	0.32
τ	12.67	7.90	36.23	4.48	2.65	12.80	1.80	1.48	5.15

our FMA for WMAP 4-years using the WMAP fiducial model. The FMA predictions for WMAP - 4years are to be compared with the recent WMAP 1-year results.

The errors in most of the other cosmological parameters are unaffected by the presence of reionization *if* one has both temperature and polarization data. If one has just one of them then the accuracy is quite different, and also it will depend on whether has high or low τ . This is because different degeneracies may be dominant in each case, while combining temperature and polarization information helps break such degeneracies.

The inclusion of the new parameter τ for a standard model reduces the accuracy in other parameters for all but the CVL experiment (and in this case for all but ω_Λ) as can be seen from a comparison of Table VI with Table II.

Comparing Tables VI (for $\tau = 0.20$) and X (for $\tau =$

0.02) an immediate effect of considering a large value of τ is to increase the accuracy on τ itself. For example the case with temperature and polarization information used jointly, the accuracy on the other parameters is not necessarily reduced by considering a larger value of τ while its accuracy remains almost the same for a CVL experiment. Whilst comparing Tables VII (for $\tau = 0.20$) and XI (for $\tau = 0.02$) the effect of a large value of τ , considering the case temperature and polarization used jointly, for WMAP is to increase the accuracy on most of the parameters particularly noticeable for the parameters α and τ ; for Planck only the accuracy on τ is improved while the other parameters have slightly worse accuracy; finally for a CVL experiment the accuracy is the same for all but ω_Λ which is slightly worse, and τ which is much better. It is interesting to note that while for WMAP a large value of τ does indeed help to improve the accuracy on most

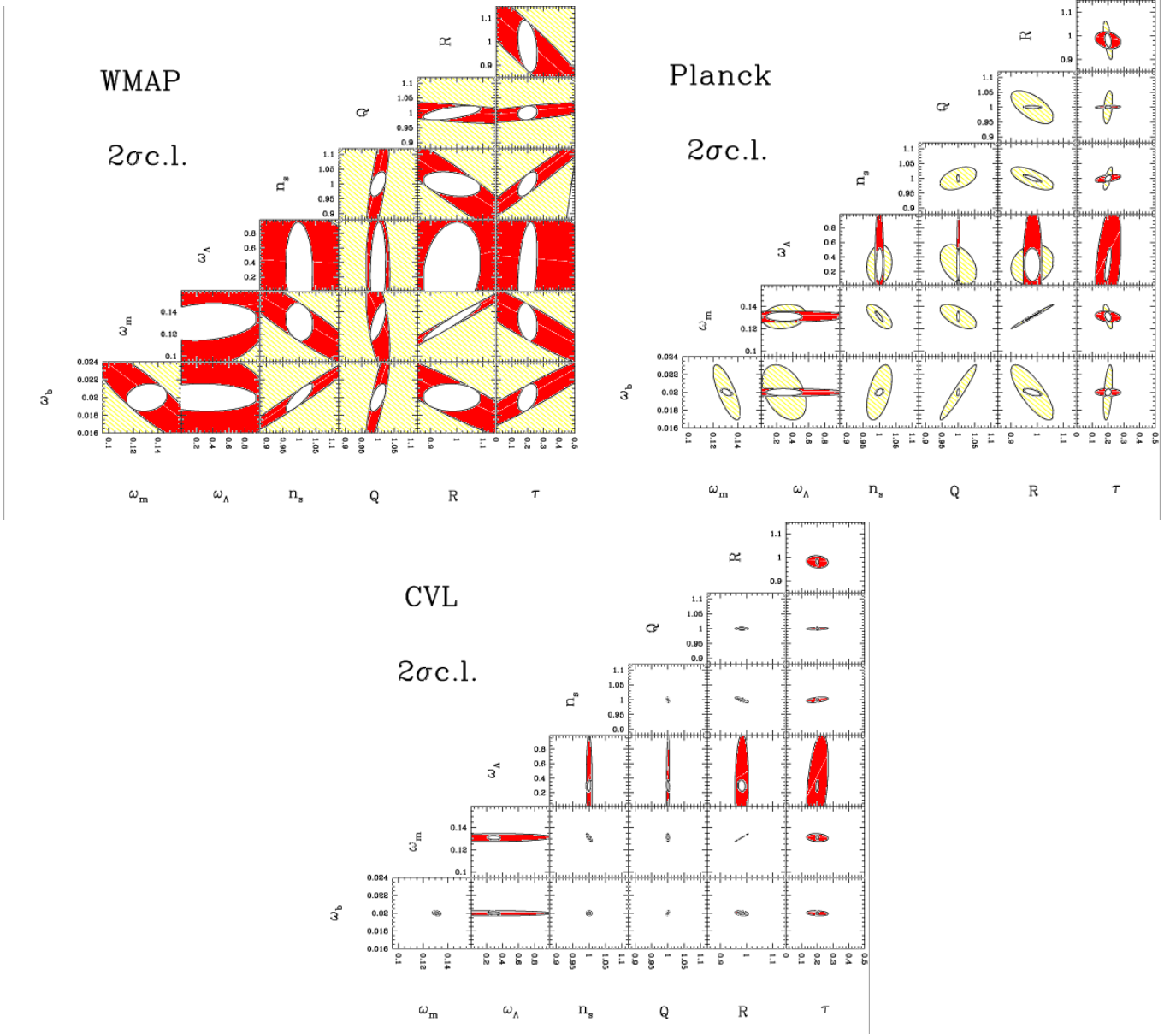


FIG. 8: Ellipses containing 95.4% (2σ) of joint confidence (all other parameters marginalized) using temperature alone (red), E-polarization alone (yellow), and both jointly (white), for a standard model with inclusion of reionization ($\tau = 0.20$).

parameters, for Planck and a CVL experiment the accuracy is improved using polarization data alone but the inverse is true using temperature data alone. Hence it is not surprising the results obtained when one considers temperature and polarization jointly.

As we go from Table XII to Table XIV the accuracy on all parameters increases as should be expected. For the WMAP - 4 years one predicts an accuracy of 3% and 11% on α and τ respectively as opposed to 4% and 14% respectively, for the 2-year mission.

The results of our forecast are that WMAP (2-years mission) is able to constrain τ with accuracy of the order 13%, which is approximately two times better than the current precision obtained from the WMAP 1-year obser-

vations, of the order of 23%. While our FMA predictions for WMAP - 4 years, gives an accuracy of the order 10% using all (TT+EE+TE) temperature, polarization and temperature-polarization cross correlation information.

Planck and a CVL experiment can constrain α with accuracies of the order 0.3% and 0.1% respectively and τ with accuracies of the order 4.5% and 1.8% respectively.

For WMAP the accuracy on τ from polarization data alone is worse by a factor of 2 than from temperature alone. On the other hand, for Planck and the CVL experiment the accuracy from polarization is better by a factor of 3 and 8 respectively, than from temperature alone. While the accuracy on α from polarization alone is worse by a factor of the order 22 and 4 than from

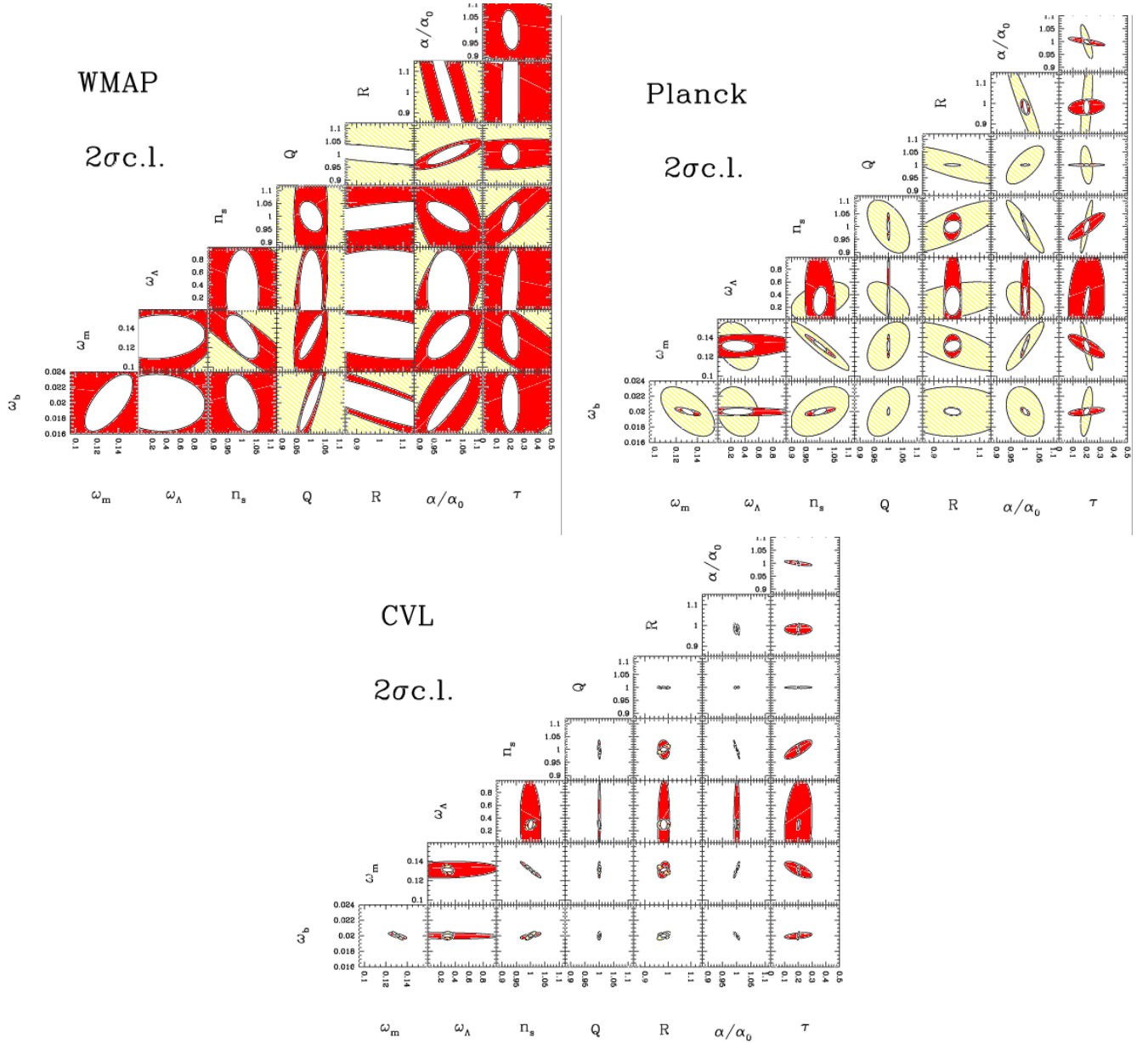


FIG. 9: Ellipses containing 95.4% (2σ) of joint confidence (all other parameters marginalized) using temperature alone (red), E-polarization alone (yellow), and both jointly (white), for a model with varying α and inclusion of reionization ($\tau = 0.20$).

temperature alone for WMAP and Planck respectively. For a CVL experiment the accuracies are similar for both polarization and temperature data alone.

The accuracy on τ obtained with Planck using Temperature data alone is roughly the same as a CVL experiment. This suggests that Planck is indeed a cosmic variance limited experiment with respect to Temperature. The inclusion of polarization the accuracy for the CVL experiment is improved by a factor of 4 when compared to Planck satellite.

B. Analysis results: Confidence contours

As before, we show in Figs. 8-10 all joint 2D confidence contours (all remaining parameters marginalized). As previously in the WMAP case the errors from E only are very large, hence the contours for T coincide almost exactly with the temperature-polarization combined case. In the CVL case it is the E contours that almost coincide with the combined ones.

From Fig. 8 without α , we can infer a good agreement between our predictions and WMAP observations. Particularly striking is the good agreement for the con-

TABLE VIII: For a model with a varying α and inclusion of reionization ($\tau = 0.20$) and the case Temperature and Polarization considered jointly. In the lines we display the components of the eigenvectors of the FM for WMAP, Planck and a CVL experiment. The quantity $1/\sqrt{\lambda_i}$ is proportional to the error along the principal direction $\mathbf{u}^{(i)}$. For each principal direction, an asterisk marks the largest cosmological parameters contribution, a dagger the second largest. Planck has errors smaller by a factor of about 5 on average than WMAP.

WMAP									
Direction i	$1/\sqrt{\lambda_i}$	ω_b	ω_m	ω_Λ	n_s	Q	\mathcal{R}	α	τ
1	2.67E-04	9.9485E-01*	-9.5907E-02†	3.4445E-06	-2.9885E-02	1.8838E-03	1.0970E-02	7.0563E-03	1.4101E-03
2	9.34E-04	7.1608E-02	7.0264E-01*	-5.5848E-04	-7.4249E-02	2.9712E-02	-1.1371E-01	-6.9403E-01†	1.2867E-02
3	2.37E-03	5.6495E-02	5.3116E-01†	7.4496E-04	2.6323E-01	-6.4191E-01*	3.8949E-02	4.8141E-01	-7.5954E-03
4	1.11E-02	1.5030E-02	-1.1183E-01	2.6785E-02	7.5467E-01*	8.1770E-02	-1.0330E-01	-1.8322E-01	-6.0506E-01†
5	1.56E-02	4.0281E-02	4.2554E-01	-1.1637E-02	1.8055E-01	7.5707E-01*	1.4249E-01	4.2651E-01†	9.5864E-02
6	2.87E-02	4.3952E-03	-1.4321E-01	-1.9274E-02	5.5866E-01†	-3.4689E-02	-1.1323E-01	-1.7258E-01	7.8942E-01*
7	1.43E-01	-8.9145E-03	-2.9306E-02	-6.9614E-02	1.0039E-01	-7.7565E-02	9.6787E-01*	-2.0293E-01†	1.3044E-02
8	2.66E-01	-4.7667E-04	3.1536E-03	9.9696E-01*	-5.9578E-04	1.0494E-03	6.9739E-02†	-8.3540E-03	3.3561E-02
Planck									
Direction i	$1/\sqrt{\lambda_i}$	ω_b	ω_m	ω_Λ	n_s	Q	\mathcal{R}	α	τ
1	9.52E-05	8.0730E-01*	-4.3681E-01†	7.2721E-05	2.1375E-03	-1.7179E-02	6.5966E-02	3.9091E-01	-2.5317E-04
2	1.44E-04	5.8762E-01*	5.8285E-01†	1.1644E-04	-3.6480E-02	-5.9816E-02	-8.5667E-02	-5.5021E-01	2.1552E-03
3	5.11E-04	3.5099E-02	6.0865E-01†	-3.5134E-05	3.5326E-01	3.4997E-01	2.8062E-02	6.1633E-01*	-1.9763E-02
4	1.89E-03	4.0108E-02	-2.1450E-01	2.1539E-03	-6.8889E-02	9.3126E-01*	-1.9318E-03	-2.8091E-01†	-3.8245E-02
5	4.95E-03	-4.2534E-03	1.0972E-01	-4.8443E-02	-4.2498E-01†	6.7120E-02	9.4317E-02	1.2132E-01	8.8140E-01*
6	1.10E-02	1.0598E-02	-2.0227E-01	-4.5823E-02	8.0262E-01*	-3.4226E-02	-2.1882E-01	-2.1656E-01	4.6553E-01†
7	1.43E-02	-1.1429E-03	6.9110E-03	-1.3268E-02	2.0966E-01†	-2.6773E-02	9.6472E-01*	-1.5502E-01	1.9638E-02
8	9.16E-02	5.2242E-05	-3.4224E-03	9.9768E-01*	1.9182E-02	-6.5898E-04	7.3693E-03	-5.4534E-03	6.4522E-02†
CVL									
Direction i	$1/\sqrt{\lambda_i}$	ω_b	ω_m	ω_Λ	n_s	Q	\mathcal{R}	α	τ
1	2.67E-05	-1.2266E-01	7.5163E-01*	8.1216E-06	-4.6840E-03	-1.6753E-03	-1.0827E-01	-6.3895E-01†	1.9959E-04
2	4.30E-05	9.8772E-01*	1.5389E-01†	4.2633E-05	2.3505E-02	-1.5836E-03	-1.1188E-02	-6.8644E-03	-5.1213E-04
3	2.27E-04	-8.6274E-02	5.2862E-01†	-2.5551E-04	3.8678E-01	4.0618E-01	2.3505E-02	6.3051E-01*	-2.1039E-02
4	1.28E-03	4.3348E-02	-2.9931E-01†	5.8579E-03	9.2070E-02	8.7287E-01*	6.9630E-03	-3.6458E-01	-7.1777E-02
5	2.70E-03	-2.8246E-03	1.2912E-01	-1.2398E-02	-6.1385E-01†	2.2772E-01	8.4123E-02	1.4231E-01	7.2606E-01*
6	3.93E-03	5.6917E-03	-1.4889E-01	-4.9020E-02	6.7866E-01†	-1.4028E-01	-2.2646E-02	-1.7680E-01	6.8071E-01*
7	5.96E-03	-1.3903E-04	5.9101E-02	5.2914E-03	5.7747E-02	-3.8594E-02	9.8992E-01*	-9.8529E-02†	-4.4876E-02
8	3.19E-02	-7.2460E-05	-4.1402E-03	9.9869E-01*	2.4943E-02	-8.8701E-03	-5.3456E-03	-4.0841E-03	4.3079E-02†

four plots in the (n_s, τ) plane which clearly exhibits the observed degeneracy [46]. For Planck the inclusion of polarization data helps to break degeneracies in particular between τ and the other parameters for example with n_s . For a CVL experiment the contours are further narrowed with the joint temperature polarization analysis in agreement with the tabulated accuracies on τ .

Again, looking at Fig. 10 with α , our predictions for the contour plots in the plane (τ, n_s) are in close agreement with the observed degeneracy [4]. This same plot shows that the degeneracy direction between α and n_s is almost orthogonal to that between τ and n_s . The net result of this is a better accuracy on α when the parameter τ is included (compare Tables III and VII) while the accuracy on τ itself remains almost unchanged with inclusion of α (compare Tables VI and VII). This is in

agreement with our discussion in section III, and quantitatively explains why our α mechanism (summarized in Fig. 2) works. The accuracy on n_s is similar to that obtained without τ (compare Tables III and VII) but gets worse with inclusion of α (compare Tables VI and VII).

In other words the inclusion of reionization helps to lift most of the degeneracies when using information from both the temperature and polarization jointly hence increasing the accuracies for the cases of interest, ie, α and τ .

C. Analysis results: Principal directions

Our previous discussion of principal directions changes completely when reionization is included, as polarization

TABLE IX: For a model with a varying α and inclusion of reionization ($\tau = 0.20$) and the case (TT) ie Temperature only. In the lines we display the components of the eigenvectors of the FM for WMAP, Planck and a CVL experiment. The quantity $1/\sqrt{\lambda_i}$ is proportional to the error along the principal direction $\mathbf{u}^{(i)}$. For each principal direction, an asterisk marks the largest cosmological parameters contribution, a dagger the second largest. Planck has errors smaller by a factor of about 5 on average than WMAP.

WMAP									
Direction i	$1/\sqrt{\lambda_i}$	ω_b	ω_m	ω_Λ	n_s	Q	\mathcal{R}	α	τ
1	2.68E-04	9.9485E-01*	-9.5954E-02†	-3.8023E-05	-2.9988E-02	1.9066E-03	1.1031E-02	6.9603E-03	1.6935E-03
2	9.35E-04	7.1581E-02	7.0263E-01*	-5.4546E-04	-7.3932E-02	2.9625E-02	-1.1370E-01	-6.9410E-01†	1.1876E-02
3	2.37E-03	5.6582E-02	5.3096E-01†	7.0218E-04	2.6304E-01	-6.4218E-01*	3.9069E-02	4.8138E-01	-6.9515E-03
4	1.23E-02	2.0318E-02	-8.8391E-02	2.0436E-02	8.6583E-01*	1.5967E-01	-1.0780E-01	-1.6237E-01	-4.2215E-01†
5	1.58E-02	3.8004E-02	4.4637E-01	-1.3439E-02	5.1628E-02	7.4470E-01*	1.6739E-01	4.5598E-01†	7.7154E-02
6	1.72E-01	-4.5506E-03	-6.9729E-02	3.1859E-01	3.0219E-01	-5.4673E-02	6.8576E-01*	-2.0902E-01	5.3419E-01†
7	2.71E-01	8.7518E-03	-4.7970E-02	-1.4708E-02	2.5961E-01	5.4289E-02	-6.4792E-01†	4.5317E-02	7.1078E-01*
8	4.26E-01	1.8060E-03	3.0947E-02	9.4746E-01*	-1.1576E-01	2.6839E-02	-2.3604E-01†	8.0201E-02	-1.5838E-01
Planck									
Direction i	$1/\sqrt{\lambda_i}$	ω_b	ω_m	ω_Λ	n_s	Q	\mathcal{R}	α	τ
1	1.05E-04	7.4727E-01*	-4.9695E-01†	-5.0448E-07	3.3342E-03	-1.0958E-02	7.3355E-02	4.3488E-01	4.5857E-04
2	1.57E-04	6.6077E-01*	5.1936E-01	-1.9827E-05	-4.4896E-02	-6.7337E-02	-7.9760E-02	-5.2983E-01†	3.8563E-03
3	5.25E-04	6.1332E-02	6.1587E-01*	1.2590E-05	3.5518E-01	3.5940E-01	2.5334E-02	6.0046E-01†	-2.0469E-02
4	1.96E-03	3.3384E-02	-2.1678E-01	-7.5551E-04	-9.5447E-02	9.2928E-01*	1.9606E-03	-2.8126E-01†	-1.0701E-02
5	1.04E-02	9.3302E-03	-2.2248E-01	1.7817E-02	8.6225E-01*	-4.7210E-02	-8.6676E-02	-2.6306E-01	-3.5733E-01†
6	1.55E-02	-3.0476E-03	4.7288E-02	1.5170E-03	4.6850E-02	-1.9767E-02	9.8892E-01*	-1.0832E-01†	-7.3922E-02
7	5.73E-02	1.9693E-03	-7.2588E-02	-1.4866E-02	3.4196E-01†	-8.5608E-04	4.6134E-02	-9.7738E-02	9.3053E-01*
8	3.30E-01	-9.4432E-05	2.6522E-03	9.9973E-01*	-1.0430E-02	1.5550E-03	7.2972E-04	3.1688E-03	2.0310E-02†
CVL									
Direction i	$1/\sqrt{\lambda_i}$	ω_b	ω_m	ω_Λ	n_s	Q	\mathcal{R}	α	τ
1	5.85E-05	6.7166E-01*	-4.8908E-01	2.0754E-07	4.0071E-02	2.8188E-02	8.0901E-02	5.4839E-01†	-1.5833E-03
2	1.16E-04	7.3358E-01*	5.4117E-01†	-1.3289E-05	5.7146E-04	-2.3329E-02	-7.2058E-02	-4.0405E-01	1.3803E-03
3	2.93E-04	-9.6933E-02	6.0597E-01†	1.5493E-05	3.5035E-01	3.5105E-01	1.0230E-02	6.1395E-01*	-1.9331E-02
4	1.72E-03	3.5113E-02	-2.1156E-01	-7.1277E-04	-7.6886E-02	9.3352E-01*	1.4161E-02	-2.7618E-01†	-1.2973E-02
5	8.45E-03	9.6096E-03	-1.9881E-01	1.4790E-02	8.6840E-01*	-6.2132E-02	1.6748E-01	-2.7495E-01	-3.1390E-01†
6	1.05E-02	-2.6411E-03	1.1073E-01	-4.8547E-03	-1.5346E-01†	-1.0584E-02	9.7974E-01*	-3.0626E-02	5.6666E-02
7	4.19E-02	1.9014E-03	-6.4709E-02	-2.4494E-02	3.0336E-01†	2.7857E-05	-2.5345E-03	-7.9100E-02	9.4706E-01*
8	2.93E-01	-7.2266E-05	1.7408E-03	9.9958E-01*	-6.2208E-03	1.5285E-03	2.2272E-03	1.7693E-03	2.8118E-02†

data helps to better constrain the fine structure constant and removes the existing degeneracies between α and τ see Table VIII

In Table VIII we display the eigenvectors and eigenvalues for WMAP, Planck and a CVL experiment when reionization is included (with $\tau = 0.20$) for Temperature and Polarization considered jointly.

Planck's errors, as measured by the inverse square root of the eigenvalues, are smaller by a factor of about 5 on average than those for WMAP. In the case of a CVL experiment's errors are smaller by a factor of about 3 on average than those for Planck.

The physical parameter τ is the largest parameter contribution to the principal direction 6 for both WMAP and Planck, and is the second largest to direction 4 for WMAP and to direction 6 and 8 for Planck. While

for a CVL experiment it becomes the main contributor for principal directions 5 and 6 and the second largest for direction 8. For 4 of the 8 eigenvectors Planck obtains a better alignment of the principal directions with the axis of the physical parameters when compared with WMAP. This indicates that the inclusion of the reionization parameter τ already helps to break degeneracies for WMAP, when we compare the number 4 in 8 against 6 in 7 for the case without reionization. On the other hand, only for 4 of the 8 eigenvectors CVL obtains a better alignment of the principal directions with the axis of the physical parameters when compared with Planck, against 6 in 7 for the case without reionization.

The physical parameter α is the second largest contributor for principal directions 2, 5 and 7 for WMAP and for direction 4 for Planck being the main contributor for

TABLE X: Fisher matrix analysis results for a standard model with inclusion of reionization (for $\tau = 0.02$): expected 1σ errors for the WMAP and Planck satellites as well as for a CVL experiment. The column *marg.* gives the error with all other parameters being marginalized over; in the column *fixed* the other parameters are held fixed at their ML value; in the column *joint* all parameters are being estimated jointly.

Quantity	1σ errors (%)								
	WMAP			Planck HFI			CVL		
	marg.	fixed	joint	marg.	fixed	joint	marg.	fixed	joint
	Polarization								
ω_b	241.44	50.73	690.54	6.36	1.01	18.18	0.48	0.25	1.38
ω_m	99.44	31.71	284.39	3.55	0.34	10.14	0.70	0.03	2.01
ω_Λ	1201.35	719.21	3435.95	39.02	33.98	111.61	11.55	10.20	33.05
n_s	125.97	19.26	360.29	1.48	0.91	4.22	0.30	0.08	0.86
Q	151.63	25.09	433.68	2.20	0.45	6.30	0.24	0.07	0.68
\mathcal{R}	87.25	22.00	249.55	3.50	0.31	10.01	0.66	0.03	1.89
τ	228.76	63.74	654.28	11.45	10.29	32.75	4.23	4.10	12.10
	Temperature								
ω_b	6.00	1.27	17.16	0.83	0.59	2.37	0.56	0.38	1.59
ω_m	8.63	0.83	24.69	1.47	0.13	4.20	1.09	0.08	3.12
ω_Λ	173.23	89.11	495.44	94.22	88.94	269.48	83.32	79.55	238.30
n_s	4.42	0.52	12.64	0.50	0.13	1.43	0.34	0.07	0.98
Q	0.90	0.35	2.58	0.19	0.10	0.55	0.17	0.07	0.49
\mathcal{R}	8.78	0.74	25.10	1.43	0.11	4.10	1.05	0.07	3.00
τ	659.96	195.96	1887.52	163.30	126.81	467.05	132.38	96.66	378.61
	Temperature and Polarization								
ω_b	2.77	1.26	7.93	0.77	0.51	2.21	0.32	0.21	0.91
ω_m	4.54	0.83	12.99	1.17	0.12	3.34	0.55	0.03	1.58
ω_Λ	109.71	87.68	313.79	32.15	31.29	91.95	10.36	9.88	29.63
n_s	1.47	0.52	4.21	0.39	0.13	1.13	0.20	0.06	0.57
Q	0.81	0.35	2.33	0.18	0.10	0.52	0.14	0.05	0.41
\mathcal{R}	4.10	0.74	11.72	1.14	0.11	3.27	0.52	0.03	1.49
τ	63.32	60.36	181.09	10.38	10.06	29.69	3.87	3.81	11.07

direction 3. For a CVL experiment it becomes the second largest for directions 1 and 7 and main contributor for direction 3 just like for Planck.

In Table IX we display the principal directions considering Temperature only. Comparing Tables IX and VIII, we conclude that for 4 of the 8 eigenvectors WMAP obtains a better alignment of the principal directions with the axis of the physical parameters when polarization is included (with similar alignment for the others). While for Planck and a CVL experiment only for 3 of the 8 eigenvectors the alignment is better (with similar alignment for the others). When polarization is included, the largest and second largest physical parameter contributors remain the same for all but for directions 6 and 7 for WMAP, directions 2,3,6 and 7 for Planck, and directions 1,4,6 and 7 for a CVL experiment. For Planck for the case with temperature only, the second largest contributor to direction 2 and 6, the physical parameter α is shifted to ω_m and n_s respectively while direction 3 becomes mainly contributed by α , when polarization is included. This

indicates that when including polarization the degeneracies with α are indeed being broken. The CVL case shows that the changes occurring with inclusion of Polarization when reionization is considered is not a simple rescaling of contributions from the physical parameters to the principal directions but a rescaling by different factors for each of these physical parameters resulting in changes of the degeneracy directions. To demonstrate that this is indeed the case let us analyse both Tables in detail for the CVL case. For instance direction 1 remains unchanged with inclusion of polarization, while for direction 2 α is the third contributor by an amount similar to ω_m but is much reduced when polarization is included. Also this direction is better aligned with ω_b when temperature and polarization are considered jointly. This indicates that inclusion of polarization helped to break the degeneracy between ω_b and α . Direction 3 remains aligned with ω_Λ for both cases. Direction 5 exchanges the largest and second largest contributions from n_s to τ when polarization is included in the analysis reducing the contribution from

TABLE XI: Fisher matrix analysis results for a model with varying α and inclusion of reionization (for $\tau = 0.02$): expected 1σ errors for the WMAP and Planck satellites as well as for a CVL experiment. The column *marg.* gives the error with all other parameters being marginalized over; in the column *fixed* the other parameters are held fixed at their ML value; in the column *joint* all parameters are being estimated jointly.

Quantity	1σ errors (%)								
	WMAP			Planck HFI			CVL		
	marg.	fixed	joint	marg.	fixed	joint	marg.	fixed	joint
	Polarization								
ω_b	569.33	50.73	1628.32	6.41	1.01	18.32	1.11	0.25	3.17
ω_m	716.71	31.71	2049.84	7.22	0.34	20.66	1.65	0.03	4.71
ω_Λ	1439.68	719.21	4117.59	42.43	33.98	121.36	12.22	10.20	34.96
n_s	299.32	19.26	856.07	3.91	0.91	11.19	0.79	0.08	2.25
Q	174.27	25.09	498.41	3.15	0.45	9.00	0.24	0.07	0.69
\mathcal{R}	419.62	22.00	1200.15	9.87	0.31	28.23	1.19	0.03	3.40
α	192.47	3.57	550.48	2.59	0.05	7.42	0.40	< 0.01	1.15
τ	875.90	63.74	2505.14	15.15	10.29	43.34	4.73	4.10	13.52
	Temperature								
ω_b	14.24	1.27	40.73	1.02	0.59	2.92	0.79	0.38	2.27
ω_m	9.93	0.83	28.41	2.94	0.13	8.42	2.23	0.08	6.37
ω_Λ	173.24	89.11	495.49	108.85	88.94	311.31	93.56	79.55	267.59
n_s	4.59	0.52	13.12	1.58	0.13	4.51	1.16	0.07	3.32
Q	2.44	0.35	6.99	0.20	0.10	0.56	0.17	0.07	0.50
\mathcal{R}	26.80	0.74	76.65	1.51	0.11	4.31	1.06	0.07	3.03
α	5.00	0.12	14.31	0.49	0.02	1.41	0.34	0.01	0.96
τ	710.55	195.96	2032.22	193.10	126.81	552.27	148.41	96.66	424.46
	Temperature and Polarization								
ω_b	9.59	1.26	27.43	0.87	0.51	2.50	0.38	0.21	1.10
ω_m	8.25	0.83	23.59	1.63	0.12	4.65	0.67	0.03	1.91
ω_Λ	120.16	87.68	343.67	32.15	31.29	91.95	10.45	9.88	29.89
n_s	2.97	0.52	8.51	0.86	0.13	2.47	0.32	0.06	0.92
Q	1.99	0.35	5.69	0.19	0.10	0.53	0.14	0.05	0.41
\mathcal{R}	19.47	0.74	55.69	1.36	0.11	3.90	0.60	0.03	1.72
α	4.32	0.12	12.34	0.31	0.02	0.89	0.11	< 0.01	0.32
τ	64.65	60.36	184.91	10.52	10.06	30.09	3.91	3.81	11.18

α . So the inclusion of polarization helps to better define a direction of degeneracy between τ and n_s by breaking the degeneracy with α . The degeneracy between Q and α is also broken by shifting the second largest contributor to direction 4 from α to ω_m . The second largest contributor to direction 7 is shifted from n_s to α when polarization is included indicating that the degeneracy between \mathcal{R} and α is now dominating over the other degeneracies with α .

D. The α - τ degeneracy

Our results clearly indicate a crucial degeneracy between α and τ . In order to study it in more detail, we have extracted the relevant results from Table VII and Fig. 10 and re-displayed them in Table XV and Fig. 11. Both of these summarize the forecasts for the precision in

determining both parameters with Planck and the CVL experiment.

It is apparent from Fig. 11 that TT and EE suffer from degeneracies in different directions, for the reasons explained above. Thus combining high-precision temperature and polarization measurements one can constrain most effectively constrain both variations of α and τ . Planck will be essentially cosmic variance limited for temperature but there will still be considerable room for improvement in polarization. This therefore argues for a post-Planck polarization-dedicated experiment, not least because polarization is, in itself, better at determining cosmological parameters than temperature.

We conclude that Planck data alone will be able to constrain variations of α at the epoch of decoupling with 0.34 % accuracy (1σ , all other parameters marginalized), which corresponds to approximately a factor 5 improve-

TABLE XII: Fisher matrix analysis results for a model with varying α and inclusion of reionization (for WMAP best fit model as the fisher analysis fiducial model, $\tau = 0.17$): expected 1σ errors for the WMAP and Planck satellites as well as for a CVL experiment. The column *marg.* gives the error with all other parameters being marginalized over; in the column *fixed* the other parameters are held fixed at their ML value; in the column *joint* all parameters are being estimated jointly.

Quantity	1σ errors (%)								
	WMAP			Planck HFI			CVL		
	marg.	fixed	joint	marg.	fixed	joint	marg.	fixed	joint
	Polarization								
ω_b	285.33	26.18	816.08	5.84	0.87	16.70	0.96	0.12	2.73
ω_m	445.06	28.16	1272.90	7.48	0.46	21.41	1.40	0.03	4.00
ω_Λ	184.17	144.61	3386.80	44.12	24.08	126.18	12.83	9.33	36.70
n_s	161.11	6.14	460.78	4.22	1.00	12.08	0.71	0.08	2.04
Q	191.24	21.06	546.95	2.91	0.55	8.32	0.25	0.07	0.73
\mathcal{R}	221.83	21.69	634.44	8.81	0.35	25.19	0.79	0.02	2.26
α	113.11	4.52	323.49	2.61	0.07	7.48	0.32	0.00	0.91
τ	336.62	11.25	962.75	9.25	3.05	26.45	2.32	1.30	6.63
	Temperature								
ω_b	18.50	0.98	52.91	0.98	0.35	2.80	0.73	0.24	2.08
ω_m	17.89	0.94	51.17	3.30	0.14	9.45	2.31	0.08	6.60
ω_Λ	149.92	83.49	428.77	107.48	83.30	307.39	94.61	74.50	270.59
n_s	9.50	0.54	27.17	2.07	0.14	5.91	1.42	0.07	4.06
Q	3.27	0.37	9.36	0.21	0.11	0.60	0.19	0.07	0.53
\mathcal{R}	34.95	0.72	99.97	1.34	0.10	3.84	0.86	0.06	2.45
α	7.95	0.13	22.75	0.59	0.02	1.69	0.37	0.01	1.06
τ	119.62	17.00	342.11	32.86	9.93	93.98	25.31	6.84	72.38
	Temperature and Polarization								
ω_b	9.15	0.98	26.18	0.84	0.32	2.39	0.37	0.11	1.07
ω_m	7.55	0.94	21.58	1.62	0.13	4.65	0.61	0.03	1.75
ω_Λ	95.34	71.51	272.68	32.24	22.94	92.22	11.80	9.21	33.76
n_s	2.58	0.54	7.39	0.93	0.14	2.67	0.33	0.05	0.94
Q	1.77	0.37	5.06	0.19	0.11	0.56	0.15	0.05	0.43
\mathcal{R}	17.55	0.71	50.19	1.19	0.10	3.42	0.49	0.02	1.40
α	3.89	0.13	11.12	0.31	0.02	0.88	0.10	< 0.01	0.30
τ	13.57	9.49	38.81	4.71	2.92	13.48	1.81	1.28	5.18

ment on the current upper bound. On the other hand, the CMB *alone* can only constrain variations of α up to $\mathcal{O}(10^{-3})$ at $z \sim 1100$. Going beyond this limit will require additional (non-CMB) priors on some of the other cosmological parameters. This result is to be contrasted with the variation measured in quasar absorption systems by Ref.[10], $\delta\alpha/\alpha_0 = \mathcal{O}(10^{-5})$ at $z \sim 2$. Nevertheless, there are models where deviations from the present value could be detected using the CMB.

VIII. CONCLUSIONS

We have presented a detailed analysis of the current WMAP constraints on the value of the fine-structure constant α at decoupling. We have found that current constraints on α , coming from WMAP alone, are as strong

as all previously existing cosmological constraints (CMB combined with additional data, e.g. coming from type Ia supernovae or the HST Key project) put together. On the other hand, we have also shown that the CMB *alone* can determine α to a maximum accuracy of 0.1% - one can only improve on this number by again combining CMB data with other observables. Note that such combination of datasets is not without its subtleties—see [23] for a discussion of some specific issues related to this case.

Hence this accuracy is well below the 10^{-5} detection of Webb *et al.* [10]. However one must keep in mind that one is dealing with much higher redshifts (about one thousand rather than a few). Given that in the simplest, best motivated models for α variation, one expects it to be a non-decreasing function of time, one finds that a constraint of 10^{-3} at the epoch of decoupling can be as constraining for these models as the Webb *et al.* results.

TABLE XIII: Fisher matrix analysis results for a standard model with inclusion of reionization (for WMAP best fit model as the fisher analysis fiducial model, $\tau = 0.17$): expected 1σ errors for the WMAP - 4 years experiment. The column *marg.* gives the error with all other parameters being marginalized over; in the column *fixed* the other parameters are held fixed at their ML value; in the column *joint* all parameters are being estimated jointly.

Quantity	1σ errors (%)					
	WMAP - 4 years					
	marg.	fixed	joint	marg.	fixed	joint
	Polarization (EE)			Temperature (TT)		
ω_b	110.64	16.58	316.44	7.33	0.81	20.96
ω_m	49.48	17.16	141.52	8.91	0.77	25.49
ω_Λ	622.34	97.58	1779.93	113.30	83.39	324.06
n_s	69.43	4.89	198.58	6.68	0.53	19.11
Q	79.22	13.51	226.58	0.90	0.32	2.58
\mathcal{R}	46.52	13.04	133.06	9.25	0.59	26.47
τ	100.84	8.21	288.40	102.72	16.70	293.79
	Temp+Pol (TT+EE)			All (TT+EE+TE)		
ω_b	2.14	0.80	6.11	2.13	0.80	6.08
ω_m	3.09	0.77	8.85	3.08	0.77	8.81
ω_Λ	90.70	63.84	259.41	86.97	62.69	248.75
n_s	1.46	0.52	4.18	1.45	0.52	4.15
Q	0.52	0.32	1.48	0.52	0.32	1.48
\mathcal{R}	2.86	0.59	8.17	2.84	0.59	8.12
τ	10.52	7.45	30.08	10.41	7.44	29.78

TABLE XIV: Fisher matrix analysis results for a model with varying α and inclusion of reionization (for WMAP best fit model as the fisher analysis fiducial model, $\tau = 0.17$): expected 1σ errors for the WMAP - 4 years experiment. The column *marg.* gives the error with all other parameters being marginalized over; in the column *fixed* the other parameters are held fixed at their ML value; in the column *joint* all parameters are being estimated jointly.

Quantity	1σ errors (%)					
	WMAP - 4 years					
	marg.	fixed	joint	marg.	fixed	joint
	Polarization (EE)			Temperature (TT)		
ω_b	173.74	16.58	496.91	14.09	0.81	40.30
ω_m	260.62	17.16	745.40	13.76	0.77	39.36
ω_Λ	637.28	97.58	1822.66	133.73	83.39	382.47
n_s	108.18	4.89	309.41	7.86	0.53	22.47
Q	96.60	13.51	276.30	2.33	0.32	6.67
\mathcal{R}	133.23	13.04	381.04	26.29	0.59	75.19
α	69.10	2.48	197.62	5.83	0.12	16.66
τ	228.69	8.21	654.07	103.86	16.70	297.05
	Temp+Pol (TT+EE)			All (TT+EE+TE)		
ω_b	7.50	0.80	21.44	7.41	0.80	21.18
ω_m	5.48	0.77	15.66	5.46	0.77	15.62
ω_Λ	91.57	63.84	261.91	87.48	62.69	250.20
n_s	2.03	0.52	5.82	2.03	0.52	5.81
Q	1.31	0.32	3.73	1.30	0.32	3.71
\mathcal{R}	14.34	0.59	41.01	14.17	0.59	40.53
α	3.08	0.11	8.80	3.05	0.11	8.71
τ	10.65	7.45	30.46	10.52	7.44	30.08

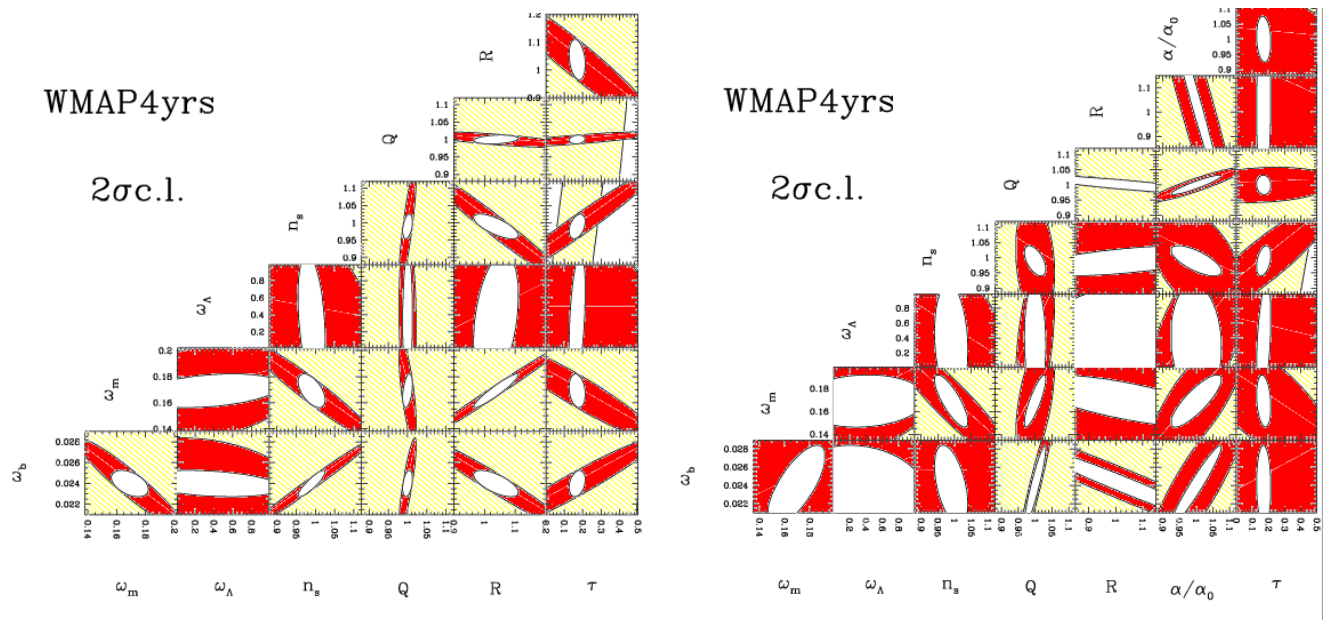


FIG. 10: Ellipses containing 95.4% (2σ) of joint confidence (all other parameters marginalized) for the WMAP - 4years, using temperature alone (red), E-polarization alone (yellow), and both jointly (white).

TABLE XV: Fisher matrix analysis results for a model with varying α and reionization: expected 1σ errors for the Planck satellite and for the CVL experiment (see the text for details). The column *marg.* gives the error with all other parameters being marginalized over; in the column *fixed* the other parameters are held fixed at their ML value; in the column *joint* all parameters are being estimated jointly.

	1σ errors (%)					
	Planck HFI			CVL		
	marg.	fixed	joint	marg.	fixed	joint
E-Polarization Only (EE)						
α	2.66	0.06	7.62	0.40	< 0.01	1.14
τ	8.81	2.78	25.19	2.26	1.52	6.45
Temperature Only (TT)						
α	0.66	0.02	1.88	0.41	0.01	1.18
τ	26.93	8.28	77.02	20.32	5.89	58.11
Temperature + Polarization (TT+EE)						
α	0.34	0.02	0.97	0.11	< 0.01	0.32
τ	4.48	2.65	12.80	1.80	1.48	5.15

In addition, there are also constraints on variations of α at the epoch of nucleosynthesis, which are at the level of 10^{-2} [22]. The main difference between them is that while CMB constraints are model independent, the BBN ones are not (they rely on the assumption of the Gasser-Leutwyler phenomenological formula for the dependence of the neutron-proton mass difference on α).

As discussed in the main text, we focused our analysis on model independent constraints, and in fact explicitly avoided discussing constraints for specific models. Nev-

ertheless it is quite easy, given the constraints (and forecasts) presented here, to translate them into constraints for the specific free parameters of one's preferred model.

We have also presented a thorough analysis of future CMB constraints on α and the other cosmological parameters, specifically for the WMAP and Planck Surveyor satellites, and compared them to those for an ideal (cosmic variance limited) experiment. Comparisons with currently published (1 year) WMAP data indicates that our Fisher Matrix Analysis pipeline is quantitatively robust and accurate.

By separately studying the temperature and polarization channels, we have explicitly shown that the degeneracy directions can be quite different in the two cases, and hence that by combining them many such degeneracies can be broken. We have also shown that in the ideal case CMB (EE) polarization is a much more accurate estimator of cosmological parameters than CMB temperature.

Nevertheless, polarization measurements are much harder to do in practice. For example, for the case of WMAP the (EE) channel will provide a quite modest contribution for the overall parameter estimation analysis. This situation is quite different for Planck: here the contributions of the temperature and polarization channels are quite similar. In fact we have also shown that Planck's temperature measurements will be almost cosmic variance limited, while its polarization measurements will be well below this ideal limit. (This fact was previously known, but it had never been quantified as was done in the present paper.) Hence this, together with the fact that polarization is intrinsically superior for the purpose of cosmological parameter estimation, make a strong case for a post-Planck, polarization-dedicated ex-

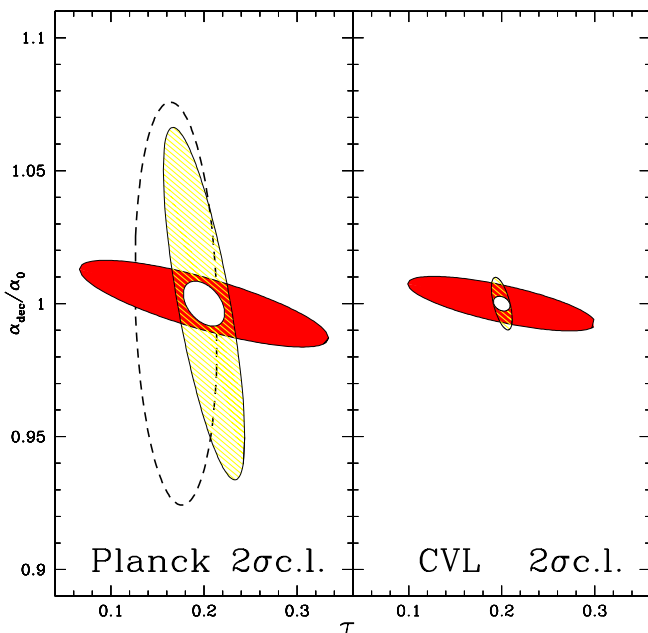


FIG. 11: Ellipses containing 95.4% (2σ) of joint confidence in the α vs. τ plane (all other parameters marginalized), for the Planck and cosmic variance limited (CVL) experiments, using temperature alone (red), E-polarization alone (yellow), and both jointly (white). The dashed contour represents the WMAP - 4years forecast using (TT+EE+TE) jointly.

periment.

Our analysis can readily be repeated for other experiments. It should be particularly enlightening to study cases of interferometer experiments and compare them with the WMAP and Planck satellites. On the other hand it would also be possible to extend it to include gravity waves, iso-curvature modes, or a dark energy

component different from a cosmological constant. However, none of these is currently required by existing (CMB and other) data, and the latter two are in fact strongly constrained.

To conclude, the prospects of further constraining α at high redshift are definitely bright. In addition, further progress is expected at low redshift, where at least three (to our knowledge) independent groups are currently trying to confirm the Webb *et al.* [10, 11, 12] claimed detection of a smaller α . All of these are using VLT data, while the original work [10, 11, 12] used Keck data. This alone will provide an important test of the systematics of the pipeline, plus in addition the three groups are using quite different methods. These and other completely new methods that may be devised thus offer the real prospect of an accurate mapping of the cosmological evolution of the fine-structure constant, $\alpha = \alpha(z)$.

Finally, a point which we have not discussed at all for reasons of space, but which should be kept in mind in the context of forthcoming experiments, is that any time variation of α will be related (in a model-dependent way) to violations of the Einstein Equivalence principle [7]. Thus a strong experimental and/or observational confirmation of either of them will have revolutionary implications not just for cosmology but for physics as a whole.

IX. ACKNOWLEDGMENTS

We would like to thank Anthony Challinor and Anthony Lasenby for useful discussions. G.R. acknowledges a Leverhulme Fellowship at the University of Cambridge, R.T. is partially supported by the Swiss National Science Foundation and the Schmidheiny Foundation and C.M. is funded by FCT (Portugal), under grant FMRH/BPD/1600/2000. This work was done in the context of the European network CMBnet, and was performed on COSMOS, the Origin3800 owned by the UK Computational Cosmology Consortium, supported by Silicon Graphics/Cray Research, HEFCE and PPARC.

-
- [1] C. L. Bennett et al. (2003), astro-ph/0302207.
 - [2] G. Hinshaw et al. (2003), astro-ph/0302217.
 - [3] A. Kogut et al. (2003), astro-ph/0302213.
 - [4] L. Verde et al. (2003), astro-ph/0302218.
 - [5] J. Polchinski (1998), Cambridge, U.K.: University Press.
 - [6] T. Damour, *Astrophys. Space Sci.* **283**, 445 (2003), gr-qc/0210059.
 - [7] C. M. Will, *Living Rev. Rel.* **4**, 4 (2001), gr-qc/0103036.
 - [8] C. J. A. P. Martins, *Phil. Trans. Roy. Soc. Lond.* **A360**, 2681 (2002), astro-ph/0205504.
 - [9] J.-P. Uzan, *Rev. Mod. Phys.* **75**, 403 (2003), hep-ph/0205340.
 - [10] J. K. Webb et al., *Phys. Rev. Lett.* **87**, 091301 (2001), astro-ph/0012539.
 - [11] J. K. Webb, M. T. Murphy, V. V. Flambaum, and S. J. Curran, *Astrophys. J. Supp.* **283**, 565 (2003), astro-ph/0210531.
 - [12] M. T. Murphy, J. K. Webb, and V. V. Flambaum (2003), astro-ph/0306483.
 - [13] A. Ivanchik, P. Petitjean, E. Rodriguez, and D. Varsshalovich, *Astrophys. Space Sci.* **283**, 583 (2003), astro-ph/0210299.
 - [14] T. Damour (2003), gr-qc/0306023.
 - [15] Y. Fujii, *Astrophys. Space Sci.* **283**, 559 (2003), gr-qc/0212017.
 - [16] H. Marion et al., *Phys. Rev. Lett.* **90**, 150801 (2003),

- physics/0212112.
- [17] T. Damour and K. Nordtvedt, *Phys. Rev.* **D48**, 3436 (1993).
- [18] D. I. Santiago, D. Kalligas, and R. V. Wagoner, *Phys. Rev.* **D58**, 124005 (1998), gr-qc/9805044.
- [19] J. D. Barrow, H. B. Sandvik, and J. Magueijo, *Phys. Rev.* **D65**, 063504 (2002), astro-ph/0109414.
- [20] K. Sigurdson, A. Kurylov, and M. Kamionkowski (2003), astro-ph/0306372.
- [21] P. P. Avelino, C. J. A. P. Martins, G. Rocha, and P. Viana, *Phys. Rev.* **D62**, 123508 (2000), astro-ph/0008446.
- [22] P. P. Avelino et al., *Phys. Rev.* **D64**, 103505 (2001), astro-ph/0102144.
- [23] C. J. A. P. Martins et al., *Phys. Rev.* **D66**, 023505 (2002), astro-ph/0203149.
- [24] C. J. A. P. Martins et al. (2003), astro-ph/0302295.
- [25] M. Zaldarriaga and U. Seljak, *Phys. Rev.* **D55**, 1830 (1997), astro-ph/9609170.
- [26] A. Kosowsky, *Ann. Phys.* **246**, 49 (1996), astro-ph/9501045.
- [27] W. Hu and M. J. White, *New Astron.* **2**, 323 (1997), astro-ph/9706147.
- [28] W. Hu, *Ann. Phys.* **303**, 203 (2003), astro-ph/0210696.
- [29] U. Seljak, *Astrophys. J.* **482**, 6 (1997), astro-ph/9608131.
- [30] M. Kamionkowski, A. Kosowsky, and A. Stebbins, *Phys. Rev. Lett.* **78**, 2058 (1997), astro-ph/9609132.
- [31] M. Kamionkowski, A. Kosowsky, and A. Stebbins, *Phys. Rev.* **D55**, 7368 (1997), astro-ph/9611125.
- [32] A. Challinor, *Phys. Rev.* **D62**, 043004 (2000), astro-ph/9911481.
- [33] J. Kovac et al., *Nature* **420**, 772 (2002), astro-ph/0209478.
- [34] S. Hannestad, *Phys. Rev.* **D60**, 023515 (1999), astro-ph/9810102.
- [35] M. Kaplinghat, R. J. Scherrer, and M. S. Turner, *Phys. Rev.* **D60**, 023516 (1999), astro-ph/9810133.
- [36] P. P. Avelino, C. J. A. P. Martins, and G. Rocha, *Phys. Lett.* **B483**, 210 (2000), astro-ph/0001292.
- [37] R. Trotta and S. H. Hansen (2003), astro-ph/0306588.
- [38] R. A. Battye, R. Crittenden, and J. Weller, *Phys. Rev.* **D63**, 043505 (2001), astro-ph/0008265.
- [39] P. P. Avelino and A. R. Liddle (2003), astro-ph/0305357.
- [40] M. Bruscoli, A. Ferrara, and E. Scannapieco (2002), astro-ph/0201094.
- [41] W. Hu and G. P. Holder, *Phys. Rev.* **D68**, 023001 (2003), astro-ph/0303400.
- [42] M. Kaplinghat et al., *Astrophys. J.* **583**, 24 (2003), astro-ph/0207591.
- [43] G. Holder, Z. Haiman, M. Kaplinghat, and L. Knox (2003), astro-ph/0302404.
- [44] E. W. Kolb and M. S. Turner, Addison-Wesley Publishing Company (1993).
- [45] D. F. Mota and J. D. Barrow (2003), astro-ph/0306047.
- [46] D. Spergel et al. (2003), astro-ph/0302209.
- [47] A. Melchiorri, L. Mersini, C. J. Odman, and M. Trodden, *Phys. Rev.* **D68**, 043509 (2003), astro-ph/0211522.
- [48] R. Bean, S. H. Hansen, and A. Melchiorri, *Phys. Rev.* **D64**, 103508 (2001), astro-ph/0104162.
- [49] H. V. Peiris et al. (2003), astro-ph/0302225.
- [50] W. H. Kinney, E. W. Kolb, A. Melchiorri, and A. Riotto (2003), hep-ph/0305130.
- [51] R. Bean, A. Melchiorri, and J. Silk (2003), astro-ph/0306357.
- [52] R. Fisher, *J. Roy. Stat. Soc.* **98**, 39 (1935).
- [53] M. Tegmark, A. Taylor, and A. Heavens, *Astrophys. J.* **480**, 22T (1997), astro-ph/9603021.
- [54] G. Jungman, M. Kamionkowski, A. Kosowsky, and D. N. Spergel, *Phys. Rev. Lett.* **76**, 1007 (1996), astro-ph/9507080.
- [55] G. Jungman, M. Kamionkowski, A. Kosowsky, and D. N. Spergel, *Phys. Rev.* **D54**, 1332 (1996), astro-ph/9512139.
- [56] L. Knox, *Phys. Rev.* **D52**, 4307 (1995), astro-ph/9504054.
- [57] M. Zaldarriaga, D. N. Spergel, and U. Seljak, *Astrophys. J.* **488**, 1 (1997), astro-ph/9702157.
- [58] J. R. Bond, G. Efstathiou, and M. Tegmark, *Mon. Not. Roy. Astron. Soc.* **291**, L33 (1997), astro-ph/9702100.
- [59] G. Efstathiou and J. R. Bond, *MNRAS* **304**, 75 (1999), astro-ph/9807103.
- [60] G. Efstathiou, *MNRAS* **332**, 193 (2002), astro-ph/0109151.
- [61] A. Melchiorri and L. M. Griffiths, *New Astron. Rev.* **45**, 321 (2001), astro-ph/0011147.
- [62] R. Bowen, S. H. Hansen, A. Melchiorri, J. Silk, and R. Trotta, *Mon. Not. Roy. Astron. Soc.* **334**, 760 (2002), astro-ph/0110636.
- [63] W. Hu and N. Sugiyama, *Phys. Rev.* **D51**, 2599 (1995), astro-ph/9411008.
- [64] W. H. Press et al. (1992).